

Anaerobic oxidation of methane by sulfate in hypersaline groundwater of the Dead Sea aquifer

N. AVRAHAMOV,¹ G. ANTLER,² Y. YECHIELI,³ I. GAVRIELI,³ S. B. JOYE,⁴ M. SAXTON,⁴ A. V. TURCHYN² AND O. SIVAN¹

¹Department of Geological and Environmental Sciences, Ben Gurion University of the Negev, Beer-Sheva, Israel

²Department of Earth Sciences, University of Cambridge, Cambridge, UK

³The Geological Survey of Israel, Jerusalem, Israel

⁴Department of Marine Sciences, The University of Georgia, Athens, GA, USA

ABSTRACT

Geochemical and microbial evidence points to anaerobic oxidation of methane (AOM) likely coupled with bacterial sulfate reduction in the hypersaline groundwater of the Dead Sea (DS) alluvial aquifer. Groundwater was sampled from nine boreholes drilled along the Arugot alluvial fan next to the DS. The groundwater samples were highly saline (up to 6300 mM chlorine), anoxic, and contained methane. A mass balance calculation demonstrates that the very low $\delta^{13}\text{C}_{\text{DIC}}$ in this groundwater is due to anaerobic methane oxidation. Sulfate depletion coincident with isotope enrichment of sulfur and oxygen isotopes in the sulfate suggests that sulfate reduction is associated with this AOM. DNA extraction and 16S amplicon sequencing were used to explore the microbial community present and were found to be microbial composition indicative of bacterial sulfate reducers associated with anaerobic methanotrophic archaea (ANME) driving AOM. The net sulfate reduction seems to be primarily controlled by the salinity and the available methane and is substantially lower as salinity increases (2.5 mM sulfate removal at 3000 mM chlorine but only 0.5 mM sulfate removal at 6300 mM chlorine). Low overall sulfur isotope fractionation observed ($^{34}\epsilon = 17 \pm 3.5\%$) hints at high rates of sulfate reduction, as has been previously suggested for sulfate reduction coupled with methane oxidation. The new results demonstrate the presence of sulfate-driven AOM in terrestrial hypersaline systems and expand our understanding of how microbial life is sustained under the challenging conditions of an extremely hypersaline environment.

Received 13 November 2013; accepted 16 June 2014

Corresponding author: O. Sivan. Tel.: 972 8 6477504; fax: 972 8 6472997; e-mail: oritsi@bgu.ac.il

INTRODUCTION

During anaerobic organic matter oxidation, microbial respiration is coupled with the reduction in series of electron acceptors that provide decreasing free energy yields. The largest energy yield is associated with nitrate reduction (denitrification), then manganese and iron reduction, followed by sulfate reduction, and finally fermentation of organic matter or the reduction of CO_2 to methane via methanogenesis (Froelich *et al.*, 1979). Due to the high concentration of sulfate in the ocean, dissimilatory bacterial sulfate reduction (Eq. 1) is responsible for the majority of organic matter oxidation in marine sediments (Kasten & Jørgensen, 2000).



When methane is available as the electron donor, microorganisms can oxidize it (methanotrophy), and in some cases, sulfate is reduced primarily by coupling with anaerobic oxidation of methane (AOM) (e.g., Niewöhner *et al.*, 1998; Boetius *et al.*, 2000; Aharon, 2000; Sivan *et al.*, 2007), as shown in Eq. 2 (Hoehler *et al.*, 1994):



Sulfate-driven AOM consumes almost all the upward fluxes of methane in marine sediments and prevents its release to the atmosphere. This process typically involves

microbial consortia of archaea and bacteria affiliated with methanosarcina-type methanogens and sulfate-reducing bacteria, respectively (Boetius *et al.*, 2000). A common view is that anaerobic methanotrophic archaea (ANME) oxidize the methane while the bacterial partner uses the resulting reducing equivalents to reduce sulfate (Thauer & Shima, 2008; Basen *et al.*, 2011). Recently, however, AOM mediated solely by archaea was reported (Milucka *et al.*, 2012); whether this process is widespread in the natural environment is unknown. Sulfate-driven AOM has also been reported in a variety of terrestrial habitats, including terrestrial mud volcanoes (e.g., Alain *et al.*, 2006), landfills (Grossman *et al.*, 2002), in the anoxic waters of a eutrophic freshwater lake (Eller *et al.*, 2005), and in anoxic coastal freshwater and brackish sediments (Segarra *et al.*, 2013). ANME sequences have also been reported from diverse soils, aquifers, and oilfield production waters, although their linkage to sulfate-driven AOM in such habitats is unclear (Knittel & Boetius, 2009).

Anaerobic oxidation of methane seems uniquely suited to extreme natural environments: AOM has been observed in temperatures of up to 75 °C in the hydrothermal sediments of the Guaymas Basin (Holler *et al.*, 2011), in CO₂-rich seep sediments with an *in situ* pH as low as 4 (Inagaki *et al.*, 2006a), in alkaline fluids of carbonate chimneys with pH values of 9–11, and in diffuse vent fluids at temperatures up to 70 °C (Brazelton *et al.*, 2006). However, documentation of AOM in hypersaline environments is limited. Thermodynamically, sulfate-driven AOM is not expected in salt-stressed environments because of the extremely low-energy yield and the high energy needed for the osmotic adaptation to the surrounding medium (Oren, 2011). Still, sulfate-driven AOM has been observed in hypersaline marine cold seep sediments (Orcutt *et al.*, 2005; Lloyd *et al.*, 2006; Maignien *et al.*, 2013). However, the occurrence of this process in continental hypersaline environments has not been reported. Here, we provide the first time geochemical evidence of AOM in the Dead Sea (DS) aquifer, which expands our understanding of how microbial life is sustained under challenging conditions of an extreme hypersaline environment.

Traditional organoclastic bacterial sulfate reduction (not associated with methane) is often observed in hypersaline terrestrial systems (e.g., Canfield & Des Marais, 1991; Brandt *et al.*, 2001; Porter *et al.*, 2007; Van der Wielen & Heijs, 2007; Murray *et al.*, 2012; Roychoudhury *et al.*, 2013). Evidence for bacterial sulfate reduction has also been observed in the highly sulfate-depleted calcium chloride brines of the DS. Comparison of the isotopic composition of sulfate and sulfide from the lower anoxic water layer during the DS meromictic stage, before the 1978 overturn (Steinhorn, 1985), pointed to bacterial sulfate reduction as the source of the sulfide because this microbially mediated process selects for ³²S over ³⁴S (Nissenbaum

& Kaplan, 1976). Sulfur isotopes and ammonium concentrations in two groups of brine along the western coast of the DS also indicate oxidation of the organic matter through bacterial sulfate reduction (Gavrieli *et al.*, 2001).

To date, no ANMEs have been identified in the DS environment; however, the potential for methanogenesis and AOM has been demonstrated. Microbial radiotracer studies of methanogenesis in sediments from the DS showed that methane is produced from methanol in sediment slurries (Marvin Di Pasquale *et al.*, 1999). In a recent study (Avrahamov *et al.*, 2010), methane was found in most hypersaline groundwaters, and from mass balance calculations of the carbon isotopic composition ($\delta^{13}\text{C}$) of the dissolved inorganic carbon (DIC), it was hypothesized that methanotrophy played an important role in this groundwater system.

The isotopic composition of sulfate and DIC in groundwater provides evidence for biogeochemical processes involving methane and sulfate due to the significant isotopic fractionations associated with their biological transformations. Depending on the extent of reaction, AOM generates highly ¹³C-depleted DIC leaving ¹³C-enriched residual methane. This fingerprinting is the result of biological fractionation during methane oxidation (ϵ ~0–10‰, Whiticar *et al.*, 1986; Whiticar, 1999). An average ϵ value of $13 \pm 9\%$ was presented by Alperin & Hoehler (2009) and the initial highly depleted $\delta^{13}\text{C}$ value of the methane itself, which is about -50‰ to -100‰ (Vienna Pee Dee Belemnite—VPDB) (Alperin *et al.*, 1988; Martens *et al.*, 1999). During bacterial sulfate reduction, a decrease of dissolved sulfate concentration coupled with isotopic enrichment of both ³⁴S and ¹⁸O in the dissolved sulfate ($\delta^{34}\text{S}_{\text{SO}_4}$ and $\delta^{18}\text{O}_{\text{SO}_4}$) is expected, because sulfate-reducing bacteria discriminate against the heavy isotope (e.g., Mizutani & Rafter, 1973; Fritz *et al.*, 1989).

This study presents geochemical and microbial evidence for sulfate-driven AOM in the aquatic, hypersaline groundwater system along the DS shore. This system includes the fresh-saline groundwater interface (FSI) from which the extremely saline samples in the alluvial fan of Wadi Arugot were taken (Fig. 1). We determined the sulfur and oxygen isotope fractionations and the apparent net sulfate reduction rate and explored the factors controlling the extent of sulfur isotope fractionation in this extreme environment.

Study site

The DS is a hypersaline terminal lake located in the deepest part of the DS Transform Fault. The salinity of the lake is ~345 g TDS/l (6400 mM Cl⁻). It is currently supersaturated with respect to gypsum (Reznik *et al.*, 2011) and halite (Reznik *et al.*, 2009), and its brine inorganically precipitates aragonite (Barkan *et al.*, 2001) and halite (Gavrieli, 1997). The DS brine has a calcium chloride

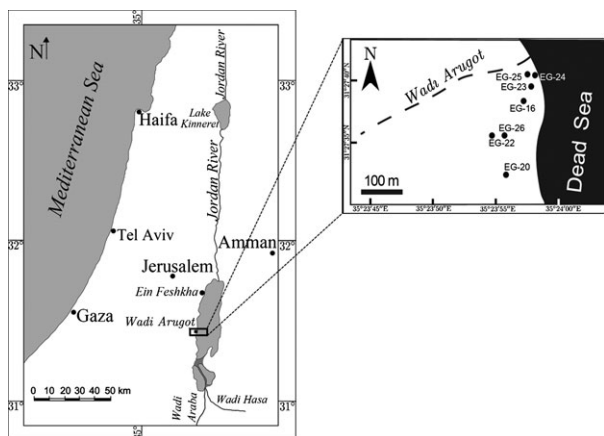


Fig. 1 Location map of the Dead Sea, Wadi Arugot, and the research borehole distribution.

composition ($\text{Na}/\text{Cl} < 1$ and $\text{Ca}/(\text{SO}_4^{2-} + \text{HCO}_3^{-}) > 1$), which is characterized by a low sulfate concentration relative to its salinity (Table 1). It was postulated that the DS brines are the result of seawater infiltration from the Mediterranean Sea in the Neogene (Neev & Emery, 1967; Zak, 1967), which underwent high evaporation and several stages of rock–water interaction (Starinsky, 1974).

The DS surface level has been dropping during the past 50 years due to human activity, with rates reaching more than 1 m year^{-1} in the last several years (Anati & Shasha, 1989; Lensky *et al.*, 2005; Yechieli *et al.*, 2010). This drop in the DS water level has further concentrated the salts and increased the salinity, causing massive precipitation of halite from the water column to the lake bottom, and to the development of sinkholes in the surrounding aquifer. The DS aquifer is an ideal site to investigate sulfate-driven AOM in a hypersaline environment, because of the high ionic strength of the DS water ($9 \text{ mol KgH}_2\text{O}^{-1}$), the relatively low sulfate concentrations ($\sim 4 \text{ mM}$ in the DS) that may therefore show large isotopic shifts, the anoxic conditions of most of the hypersaline groundwater, and the presence of methane (Avrahamov *et al.*, 2010).

The hydrological system in the Dead Sea aquifer

Two main aquifers exist in the western part of the DS rift: the limestone and dolomite layers of the Judea Group of Upper Cretaceous age, and the Quaternary alluvial aquifer (Fig. 2) (Arad & Michaeli, 1967; Yechieli *et al.*, 1995). This study focuses on the FSI in the alluvial aquifer with the DS, which consists of clastic deltaic (gravel, sand, and clay) and lacustrine (clay, aragonite, gypsum, and salt) sediments of the Lisan and Zeelim formations. Alternations between gravel and clay create several subaquifers that differ in their groundwater level, temperature, and chemical composition (Yechieli, 2006). The alluvial aquifer is generally

separated from the Cretaceous aquifer by the western marginal faults of the DS rift, which sets the Cretaceous limestone rocks of the Judea Group against the Quaternary alluvial rocks. Due to the low precipitation and high evaporation rates in the DS area, only a small amount of water penetrates directly to the alluvial aquifer from floods. The main freshwater source of the alluvial aquifer is the Cretaceous aquifer from which water flows through the noted fault zone. The Cretaceous aquifer freshwater emerges in several springs along the western faults of the DS rift, such as the Ein Gedi spring.

The groundwater flow in the DS alluvial aquifer is presented in a schematic hydrogeological cross section (Fig. 2), showing that the groundwater in the upper phreatic aquifer has two opposite paths. Due to the hydraulic gradient in the region, the general groundwater flow is from the highlands from the west to the east. On the other hand, beneath the FSI zone, there is saline water circulation from the DS inland despite the fact that the water level in the DS is decreasing (Kiro *et al.*, 2008; Avrahamov *et al.*, 2010). In the FSI zone itself, the hypersaline groundwater mixes with the relatively fresh groundwater, generating continuous seaward outflow of saline water. In general, there are three main water bodies in the DS aquifer (Lewenberg, 2005; Kiro, 2007): (i) fresh groundwater in the west, at the foot of the Judean desert mountain ($\text{TDS} > 1 \text{ g L}^{-1}$); (ii) groundwater with chemical characteristics similar to that of the DS in the east (hereafter called DS circulating groundwater); and (iii) unique brines which are different from the DS brine in their chemical composition (Na/Cl , Mg/K , and Ca/Mg) and salinity in the west (hereafter called western brine). In the first stage of groundwater mixing, the fresh groundwater flows eastward toward the western brine, causing dilution of the latter. Later, the western brine flows toward the lake and mixes with the DS water. It seems thus that at the Arugot alluvial fan, there is no direct flow of freshwater above the brines toward the DS (Kiro, 2007). The boundary between DS circulating water and the two other water bodies (western brine and fresh water) forms the FSI. The brine in the lower subaquifer below the upper aquifer is somewhat different. This research focuses on the anoxic part of the FSI zone in the upper aquifer. This is the more saline part of the FSI ($> 1600 \text{ mM Cl}^-$), where the two end members of the hypersaline groundwaters are the western brine and the DS water.

METHODS

Sampling and field procedure

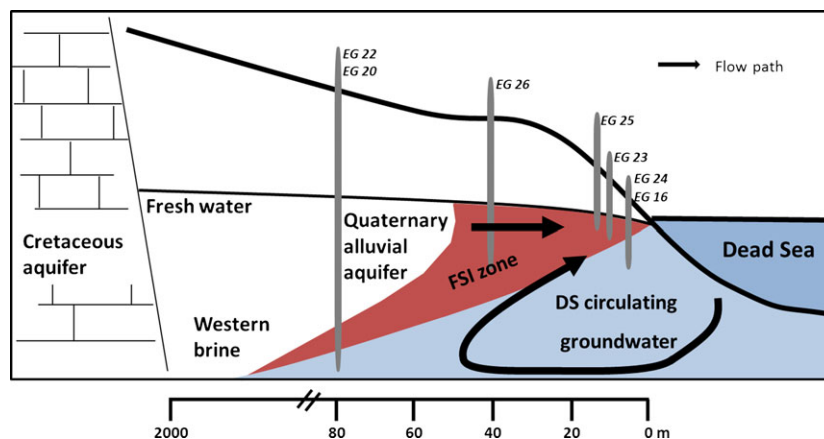
Water samples were collected from nine boreholes drilled along the Arugot alluvial fan next to the DS (Fig. 1). Groundwater samples were collected with a submersible

Table 1 Chemical and isotopic compositions of the DS and groundwater and their group affiliation; Dead Sea water (DS), freshwater (FW), western brine (WB), lower subaquifer (LA), and mixed water of the DS and the western brine (BD). Gypsum saturation state (Ω_{gyp}) was calculated using the PhreeQC code

Sample	Water group	Date m.d.y	pH	Na ⁺ mM	Ca ²⁺ mM	Mg ²⁺ mM	Cl ⁻ mM	SO ₄ ²⁻ mM	Fe ²⁺ mM	DIC mM	DO μM	H ₂ S μM	CH ₄ μM	$\delta^{18}\text{O}_{\text{SO}_4}$ † ‰ (VSMOW) ±0.4‰	$\delta^{34}\text{S}_{\text{SO}_4}$ ‡ ‰ (VCDT) ±0.4‰	$\delta^{13}\text{C}_{\text{DIC}}$ † ‰/PDB	$\delta^{13}\text{C}_{\text{CH}_4}$ † ‰/PDB	Ω_{gyp}
DSW*	DS	1983	–	1662	444	1814	6290	4.55	–	–	–	–	–	–	–	–	–	1.3
DSW†	DS	1.31.12	6.0	1435	449	1872	6346	4.07	2	0.98 ± 0.02	43 ± 2	–	–	13.65	15.90	2.8	–	1.4
EG20/55‡	DS	11.26.7	5.6	1605	422	1849	6377	–	–	1.87	–	–	228	–	–	–17.0	–	–
EG20/55	DS	2.1.12	5.6	1554	400	1761	6172	2.46 ± 0.10	22	2.30 ± 0.03	–	<7	38	16.6	21.9	–14.7	–	0.6
EG24/10	DS	2.1.12	5.9	1319	436	1894	6284	2.87 ± 0.04	2	0.77 ± 0.01	5	<7	0	12.6	15.8	–3.3	–37.8	0.7
EG24/19	DS	2.1.12	5.8	1333	456	1965	6319	2.52 ± 0.03	–	0.77 ± 0.02	3	<7	37	11.76	14.1	–0.8	–44.5	0.7
EG16/11‡	DS	3.7.7	5.3	1393	408	1829	5965	–	–	0.57	–	–	–	–	–	–10.2	–	–
EG22/19.7	WB	1.31.12	6.4	428	98	278	1170	30.97 ± 0.28	7	6.96 ± 1.01	0	126	41	14.6	15.8	–11.8	–	1.0
EG22/22	BD	1.31.12	6.1	1041	203	719	2976	17.14 ± 0.09	16	3.06 ± 0.14	0	<7	67	17.9	19.9	–13.3	–43.4	0.9
EG22/25‡	BD	11.26.7	5.7	1687	373	1548	5642	–	–	1.8	–	–	270	–	–	–14.1	–	–
EG22/25§	BD	6.13.10	–	1427	324	1229	4758	6.99 ± 0.03	–	–	–	–	–	19.3	22.4	–	–	1.0
EG22/29	BD	1.31.12	5.8	1501	315	1253	4755	6.46 ± 0.12	21	1.05 ± 0.02	0	<7	63	18.1	22.5	–15.3	–42.3	0.8
EG15/19‡	DS	1.10.7	5.9	1724	375	1853	5829	–	–	0.60	–	–	–	–	–	–15.4	–	–
EG26/22	BD	2.1.12	6.1	1343	262	998	4013	9.78 ± 0.03	–	2.34 ± 0.04	–	<7	59	18.0	21.4	–15.0	–36.4	0.8
EG23/6.32	DS	13.6.11	–	1635	386	1489	5528	4.72	–	2.34 ± 0.01	–	<7	0	16.4	19.4	–13.9	–	0.9
EG19/50	LA	2.1.12	6.2	529	122	331	1501	7.41 ± 0.05	0	4.09 ± 0.09	0	559	70	13.7	17.7	–8.5	–41.6	0.3
EG19/58	LA	2.1.12	7.5	940	223	657	2776	8.89 ± 0.06	–	1.05 ± 0.02	0	1941	82	17.5	23.9	–11.6	–	0.5
EG25/4.5	BD	13.6.11	6.4	1301	304	1103	4259	10.02	–	2.94 ± 0.14	–	<7	45	16.3	18.8	–13.5	–43.5	1.0
Ein Arugot	FW	5.12.07	–	2.53	1.33	1.11	2.83	0.49	–	3.53	–	–	–	–	–	–9.4	–	–

* Gavrieli (1997). †SO₄ concentration from Reznik *et al.* (2009). ‡Avrahamov *et al.* (2010). §Major elements and sulfate concentration from Kiro, unpublished data.

Fig. 2 Schematic hydrogeological cross section through the two main aquifers in the western part of the Dead Sea area (after Kiro, 2007), showing the groundwater flow directions and the three main water bodies discussed in this work; the fresh groundwater, the DS circulating groundwater in the east and the western brine. In the FSI zone, there is a mixture between the DS water to the western brine.



pump after three volumes of well water were removed. The density was measured in the field using a Paar digital DMA-35 density meter. Conductivity, pH, and temperature were also measured in the field using a portable multiparameters instrument (Multi 3500i, WTW, Weilheim, Germany). Sulfide was precipitated in the field as ZnS by adding 1–2 mL 1 M Zn-acetate to 1-L sampling bottles prior to sampling. Due to the high ionic strength of the DS, dissolved oxygen was measured in the field using a modified Winkler titration method (APHA, American Public Health Association, American Water Works Association & Pollution Control Federation, 1985; Nishri & Ben-Yaakov, 1990). Samples for major ion concentrations were collected in plastic bottles. Subsamples for total alkalinity (TA), DIC, and carbon isotope analyses were immediately filtered through 0.45- μm filters and transferred into 20-mL pre-poisoned syringes (HgCl_2 powder) to terminate bacterial activity. For methane analyses, 5 mL subsamples were transferred immediately to a vacutainer for headspace measurements. For the isotopic analyses of sulfur and oxygen of sulfate, sulfate was precipitated in the field from the groundwater as BaSO_4 , using a saturated barium chloride solution. Samples for molecular biological analyses were filtered onto 0.2 μm Sterivex filters (EMD Millipore, Billerica, MA, USA), immediately frozen at (-20°C), and stored at -80°C until DNA extraction.

Analytical methods

Na^+ , K^+ , Ca^{2+} , Mg^{2+} , Ba^{2+} , and Sr^{2+} were analyzed using inductively coupled plasma atomic emission spectroscopy (ICP-AES). Cl^- was measured by a potentiometric titration method, using silver and calomel electrodes with AgNO_3 as the titrant. The precision of the analysis of all the major elements was $\pm 2\%$, except for sulfate, which is described below. Total alkalinity was measured by titration, with 0.01 N HCl as a titrant (Metrohm model 785, Herisau, Switzerland). The analytical precision from duplicates was 0.03 meq L^{-1} . Sulfate concentrations were measured

using a Dionex DX500 high-pressure liquid chromatography (HPLC) with an external error of 0.4–4.2% between duplicates for samples (1σ). About 0.2 mL of each groundwater sample was transferred into a He-flushed vial containing H_3PO_4 for the headspace measurements of $\delta^{13}\text{C}_{\text{DIC}}$ by conventional isotopic ratio mass spectrometer (IRMS, DeltaV Advantage; Thermo, Waltham, MA, USA) with a precision of $\pm 0.1\%$. DIC concentration was also calculated from the IRMS results according to the peak height and a calibration curve (by standard samples prepared from NaHCO_3 with known DIC concentration) with an error of ± 0.2 mM.

Methane concentrations were measured by a gas chromatograph (GC, Thermo) equipped with a Shin Carbon-packed column with precision of ± 2 μM . The $\delta^{13}\text{C}_{\text{CH}_4}$ values were measured via the IRMS equipped with a PreCon interface after oxidation to CO_2 . The precision of the measurements was $\pm 0.5\%$, and the results are reported vs. the PDB standard. Total sulfide concentration was measured by titration with 5 mM thiosulfate, with an estimated error of 14 μM . Ferrous iron was fixed immediately using a ferrozine solution, and the absorbance at 562 nm was measured on a spectrophotometer (Stookey, 1970); concentrations were determined by comparison with a standard curve, and the error was less than 7 μM . The sulfur and oxygen isotope composition of the sulfate was analyzed at the University of Cambridge. Sulfate was precipitated as barite and pyrolyzed at 1450°C in a temperature conversion element analyzer (TC/EA), and the resulting carbon monoxide (CO) was measured by continuous-flow GS-IRMS (Delta V Plus) for its $\delta^{18}\text{O}_{\text{SO}_4}$. For the $\delta^{34}\text{S}_{\text{SO}_4}$ analysis, the barite was combusted at 1030°C in a flash element analyzer (EA), and the resulting sulfur dioxide (SO_2) was measured by continuous-flow GS-IRMS (Thermo, Delta V Plus). Samples for $\delta^{18}\text{O}_{\text{SO}_4}$ were run in replicate, and the standard deviation of these replicate analyses was used as the external reported error ($\sim 0.5\%$). The $\delta^{18}\text{O}_{\text{SO}_4}$ values are reported vs. VSMOW and corrected for two barite standards of known $\delta^{18}\text{O}_{\text{SO}_4}$ that

were run at the beginning and end of each set of samples (NBS 127 $\delta^{18}\text{O}_{\text{SO}_4} = 8.6\text{‰}$ and EM barite $\delta^{18}\text{O}_{\text{SO}_4} = 15\text{‰}$). $\delta^{34}\text{S}_{\text{SO}_4}$ results are reported vs. the Canyon Diablo Troilite (VCDT), and the error was determined using the standard deviation of the standard (NBS 127) at the beginning and the end of each run ($\sim 0.4\text{‰}$). The $\delta^{34}\text{S}_{\text{SO}_4}$ was also corrected to two standards of known sulfur isotope composition, NBS 127 (20.3‰) and EM barite (12‰).

DNA extraction

Groundwater samples for DNA sequence analysis were extracted via phenol–chloroform DNA extraction (Sambrook & Russell, 2001). DNA extraction was repeated four times on each filter and pooled prior to purification. Samples were purified using the Genomic DNA Clean and Concentrator Kit (Zymo Research Co., Irvine, CA, USA).

16S amplicon sequencing and analysis

16s rRNA gene hypervariable region V4–V5 from the bacterial and archaeal communities was sequenced on an Illumina MiSeq sequencer (Illumina Inc. San Diego, CA, USA) at the Josephine Paul Bay Center, Marine Biological Laboratory (MBL) in Woods Hole, Massachusetts, USA. Sample preparation, including primers used, PCR conditions, and cycling conditions are described at length on the MBL Web site (<http://vamps.mbl.edu/resources/primers.php>). Sequence QC and analyses were performed through the Visualization and Analysis of Microbial Population Structure (VAMPS) Web site (<http://vamps.mbl.edu/index.php>) and as described by Huse *et al.* (2007) and Sogin *et al.* (2006). Briefly, sequences of low quality, including sequences less than 50 bp in length, those with ambiguous taxonomic classifications, and those that did not include a forward primer sequence, were removed. Sequences were then screened for the presence of chimeric sequences using UCHIME (Edgar *et al.*, 2011). Taxonomic designations were made using GAST (Global Alignment for Sequence Taxonomy) as described by Sogin *et al.* (2006). In this process, sequences are BLAST (Altschul *et al.*, 1990) searched against the SILVA SSU database (Quast *et al.*, 2013) and MUSCLE aligned (Edgar, 2004) to the top 100 BLAST hits. Consensus taxonomy is then determined and applied to each sequence. Sequences were assigned to operational taxonomic units (OTUs) at a 3% dissimilarity cutoff in QIIME 1.7.0 (Caporaso *et al.*, 2010) using UCLUST (Edgar, 2010).

QIIME was also used to perform OTU rarefaction and richness analyses. All sequences are available via the VAMPS webpage <http://vamps.mbl.edu/> listed as SBJ_BME_Av4v5 and SBJ_BME_Av4v5. The sequences have been submitted to the NCBI short-read sequence archive.

RESULTS

Full chemical and isotope data are presented in Table 1. Based on a plot of Na^+ vs. Cl^- , the collected water samples were mixtures of the fresh groundwater (represented by the fresh spring water) and DS brines (best represented by the 1980s DS water, Fig. 3A). However, as the sulfate concentration of the DS brine is low, another end member can be distinguished—the western brine, as presented in Fig. 3B and described hereafter. The continuous drop in the DS level since the 1970s has been accompanied by a change in the chemical composition of the DS. Due to halite precipitation and mixing with end brines released from the DS potash industries, the Na/Cl ratio in the DS has decreased from 0.30 to 0.21, while Mg/K ratio increased from 9 to 9.8 (Gavrieli, 1997; Reznik *et al.*, 2009). As the chloride concentration in the DS is significantly higher than the sodium concentration (6300 mM vs. 1400 mM, respectively), during halite precipitation, sodium concentration decreases, whereas chloride concentration essentially remains constant. The behavior of these ions (sodium and chloride) in the aquifer, which is under-saturated with respect to halite, is expected to be conservative.

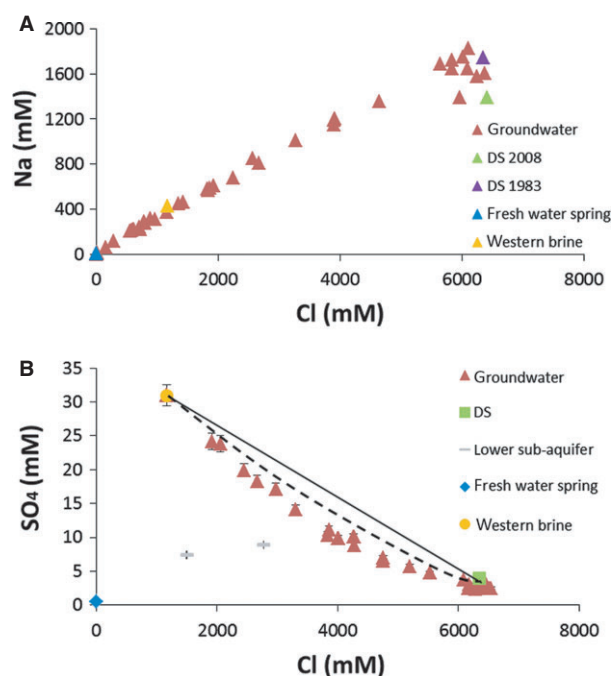


Fig. 3 (A) Na^+ and (B) SO_4^{2-} vs. Cl^- concentrations. (A) points to simple mixing between the two end members; the DS of the 80s and the fresh water spring (DS data from Gavrieli, 1997; Reznik *et al.*, 2009). The error is smaller than the symbols. (B) shows a nonlinear relationship between SO_4^{2-} and Cl^- in groundwater samples between the two end members, the DS water and the western brine. The theoretical mixing line is exhibited by a solid line. The dashed line is the predicted SO_4^{2-} concentration at saturation with gypsum ($\Omega_{\text{gyp}} = 1$) calculated from PhreeQC (Parkhurst & Appelo, 2007). Most of the groundwater samples fall below the two lines, suggesting partial removal of SO_4^{2-} by BSR.

On the other hand, the carbon system, which was studied mainly through measurements of DIC, $\delta^{13}\text{C}_{\text{DIC}}$, and alkalinity, exhibits non-conservative behavior (Avrahamov *et al.*, 2010).

Dissolved oxygen (DO)

Theoretical calculations of oxygen solubility in hypersaline solutions such as the DS brine are difficult due to the uncertainty in the formulation of the interactions of the electrolytes at high ionic strength (Nishri & Ben-Yaakov, 1990). Dissolved oxygen concentration in the DS, measured using the modified Winkler titration method, was $43 \pm 2 \mu\text{M}$, which is comparable to previous measurements ($45 \mu\text{M}$, Nishri & Ben-Yaakov, 1990). The dissolved oxygen concentrations of the groundwater in the alluvial aquifer varied from saturation to below detection. In general, most of the low salinity groundwater ($<1600 \text{ mM Cl}^-$) was oxic, whereas the hypersaline groundwater was characterized by low ($<5 \mu\text{M}$) to below detection levels of oxygen.

Dissolved sulfate and sulfide

The dissolved sulfate concentration of the DS at the time of the study was 4.1 mM . Even at this low concentration (15% of seawater concentrations), the DS is oversaturated with respect to gypsum (Reznik *et al.*, 2009). The DS water percolating into the alluvial aquifer was further depleted in sulfate relative to the DS water, with sulfate concentrations being in the range of $2.5\text{--}2.9 \text{ mM}$. The highest sulfate concentration, 31 mM , was found in the sample of lowest chloride concentration within the group of the higher salinity (Fig. 3B). In general, the sulfate concentration of this group of groundwater in the FSI zone decreases with increasing salinity and exhibits depletion from both the expected mixing values between the DS and the western brine (represented by borehole EG22/19.7 values, Table 1), as well as from the predicted sulfate concentration at saturation with respect to gypsum ($\Omega_{\text{gy}} = 1$, Fig. 3B). Exceptions to this were the samples from the lower subaquifer that are distinguished by their ion ratios and salinity and therefore were defined as a separate water body (Fig. 3B).

The expected sulfate concentration of the groundwater samples in the FSI zone, prior to any geochemical reaction, was calculated by the mixing fraction of the DS end member (f_{DS}) according to the following equation:

$$f_{\text{DS}} = \frac{\text{Cl}_{\text{sample}} - \text{Cl}_{\text{wb}}}{\text{Cl}_{\text{DS}} - \text{Cl}_{\text{wb}}} \quad (3)$$

where $\text{Cl}_{\text{sample}}$ is the chlorine concentration in the measured sample, and Cl_{wb} and Cl_{DS} are the chlorine concentrations in the two saline end members the western brine

(wb) and the DS, respectively. Due to halite precipitation in some of the groundwater samples, the mixing fractions for them (EG22/22 and EG22/25.3) were calculated using the magnesium concentration instead of chloride concentration. The calculated sulfate concentrations in the groundwater were then compared with the expected sulfate concentration at gypsum saturation ($\Omega_{\text{gy}} = 1$). The latter were calculated using the PhreeqC code (Parkhurst & Appelo, 2007) and its Pitzer database for high ionic strength solutions. The code 'precipitates' gypsum from the oversaturated brine until the brine attains saturation with respect to gypsum.

The aqueous geochemistry of the groundwater samples from the lower subaquifer indicates that these samples have some unique brine component, in addition to the western brine. As there are not enough data on the lower subaquifer, the pre-reaction sulfate and $\delta^{34}\text{S}_{\text{SO}_4}$ values cannot be calculated, and these samples were excluded from the isotopic mass balance calculations.

Most of the groundwater samples contained low concentrations of sulfide (Table 1), but the low resolution of the sulfide measurements did not permit identification of a trend. However, sulfide concentrations in the western brine and in the lower subaquifer samples differed significantly, being about 130 and $1940 \mu\text{M}$, respectively.

Methane

Methane was found in most of the hypersaline groundwater samples at concentrations of up to $82 \mu\text{M}$. The $\delta^{13}\text{C}_{\text{CH}_4}$ ranged between -36 and -44‰ (Table 1).

Fe²⁺

The concentrations of ferrous iron in some groundwater samples were measured and show depletion upon entrance to the aquifer (1.87 nM in the DS compared with 0.33 nM in groundwater 5 m from the DS) and then an increase to 19.9 nM at a distance of 80 m into the aquifer (Table 1).

Sulfur and oxygen isotope compositions in sulfate

The isotopic composition of sulfate in the groundwater ranged from 11.7‰ to 18.1‰ for the $\delta^{18}\text{O}_{\text{SO}_4}$ (‰ VSMOW) and from 14.1‰ to 23.9‰ for $\delta^{34}\text{S}_{\text{SO}_4}$ (‰ VCDT). Most of the groundwater samples were isotopically heavier than those of the modern DS ($\delta^{34}\text{S}_{\text{SO}_4} = 15.9\text{‰}$ and $\delta^{18}\text{O}_{\text{SO}_4} = 13.7\text{‰}$). An inverse correlation was observed between the sulfur and oxygen isotopic composition of sulfate and the sulfate concentration for most of the samples (Fig. 4), which suggests bacterial sulfate reduction, whereby the remaining sulfate progressively becomes enriched in the heavy sulfur and oxygen isotope as sulfate reduction proceeds. Two of the groundwater

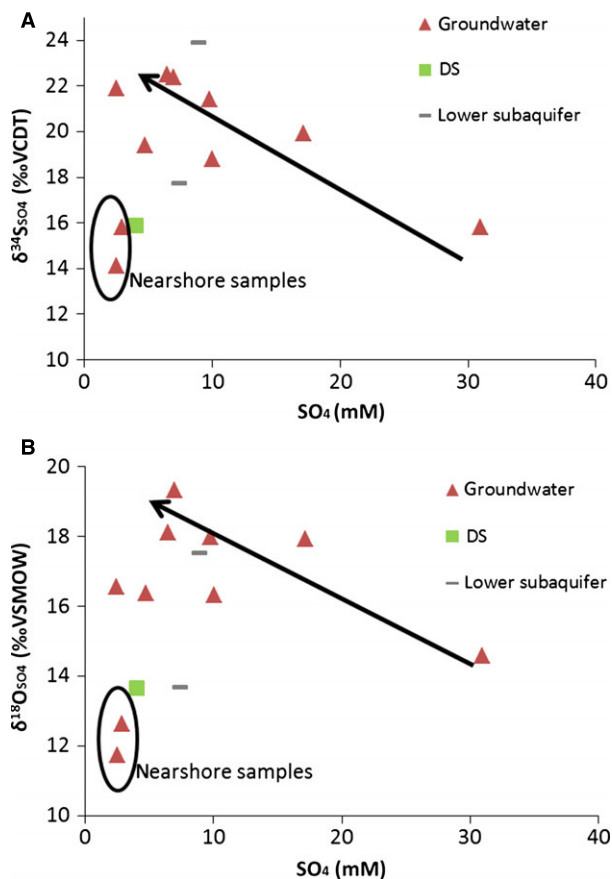


Fig. 4 (A) $\delta^{34}\text{S}_{\text{SO}_4}$ and (B) $\delta^{18}\text{O}_{\text{SO}_4}$ vs. sulfate concentrations. The two samples with values close to those of the DS are located only a few meters from the shoreline and are probably DS brines that only recently penetrated into the coastal area. The analytical error is smaller than the symbol.

samples deviate from the general trend. These samples were found very near the DS shoreline and have a similar chemical composition to that of the DS and thus probably represent intrusion of the DS brine into the coastal aquifer with only minor reaction (as discussed below).

Microbial results

To examine the microbial community potentially involved in AOM and bacterial sulfate reduction in the DS aquifer, 16s rRNA gene amplicons were sequenced from the archaeal and bacterial communities present at EG 19-50 m and EG 20-55 m (Table 2, Fig. 5). Between 22 226 and 44 449 unique sequences were obtained in the four libraries with Good's coverage estimate over 99% in each library (Table 2). Bacterial libraries at both sites were more diverse than the archaeal counterparts, with more than 800 OTUs in both bacterial libraries and 309 or fewer in both archaeal libraries (Table 2). Shannon index values from the libraries agree with the OTU results (Table 2).

Table 2 The abundance of unique sequences, OTUs grouped at 97% similarity and richness, diversity and coverage statistics calculated using the OTUs

	Unique sequences	OUT	Chao1 richness	Shannon index	Good's coverage
EG19-50 m					
Bacteria	44449	858	929.2	7.6	99.5%
Archaea	29484	208	405.2	6.25	99.8%
EG20-55 m					
Bacteria	22226	816	1059.2	7.33	99.1%
Archaea	30906	309	720.8	5.59	99.4%

DISCUSSION

DIC and $\delta^{13}\text{C}_{\text{DIC}}$ evidence for methane oxidation

It has previously been suggested that methane oxidation occurs in the DS alluvial aquifer (Avrahamov *et al.*, 2010), based on methane concentration and DIC-carbon isotope mass balance. This mass balance showed that the low $\delta^{13}\text{C}_{\text{DIC}}$ in the circulating DS groundwater and in the FSI zone, which only differ slightly in their DIC concentrations, was likely due to AOM. Here, we augment these data with oxygen concentration measurements, additional measurements of methane and sulfate concentrations, and stable isotopes of the sulfate in the anoxic aquifer. These measurements support the conclusion that AOM occurs in the DS alluvial aquifer and that it takes place at significant rates.

Mass balance calculations were performed to understand the evolution of isotopic signatures in the DS reservoir. Using these calculations, we explored four scenarios (Table 3). The ultimate objective was to track a parcel of DS water with known DIC concentration and elucidate the main processes affecting the DIC and $\delta^{13}\text{C}_{\text{DIC}}$ values when the DS water enters the aquifer. The mass balance calculation assumes that the initial DIC concentration and $\delta^{13}\text{C}_{\text{DIC}}$ value of the hypersaline groundwater were similar to that of the current DS (i.e., 0.98 mM and 2.8‰, respectively). Limited dilution of the DS groundwater by the freshwater coming from the west that flows on top of the circulating DS water does exist, but it has no significant effect on the DIC and $\delta^{13}\text{C}_{\text{DIC}}$ of the DS groundwater as the DS fraction is overwhelming. (according to mixing fraction calculation, the mixing fraction of the DS end member is 0.97–0.99.) The excess in DIC in the groundwater is then attributed to either organic matter oxidation ($\delta^{13}\text{C}_{\text{OM}} \sim -25\text{‰}$) or methane oxidation ($\delta^{13}\text{C}_{\text{CH}_4} \sim -40\text{‰}$), assuming no carbon isotope fractionation in the oxidation process. The four examples in Table 3 suggest that methane oxidation is the main source of the isotopically depleted DIC in two of them. The first two samples (EG15/19 and EG16/11 sites) have DIC lower than that of the DS with significantly lighter $\delta^{13}\text{C}_{\text{DIC}}$, implying that

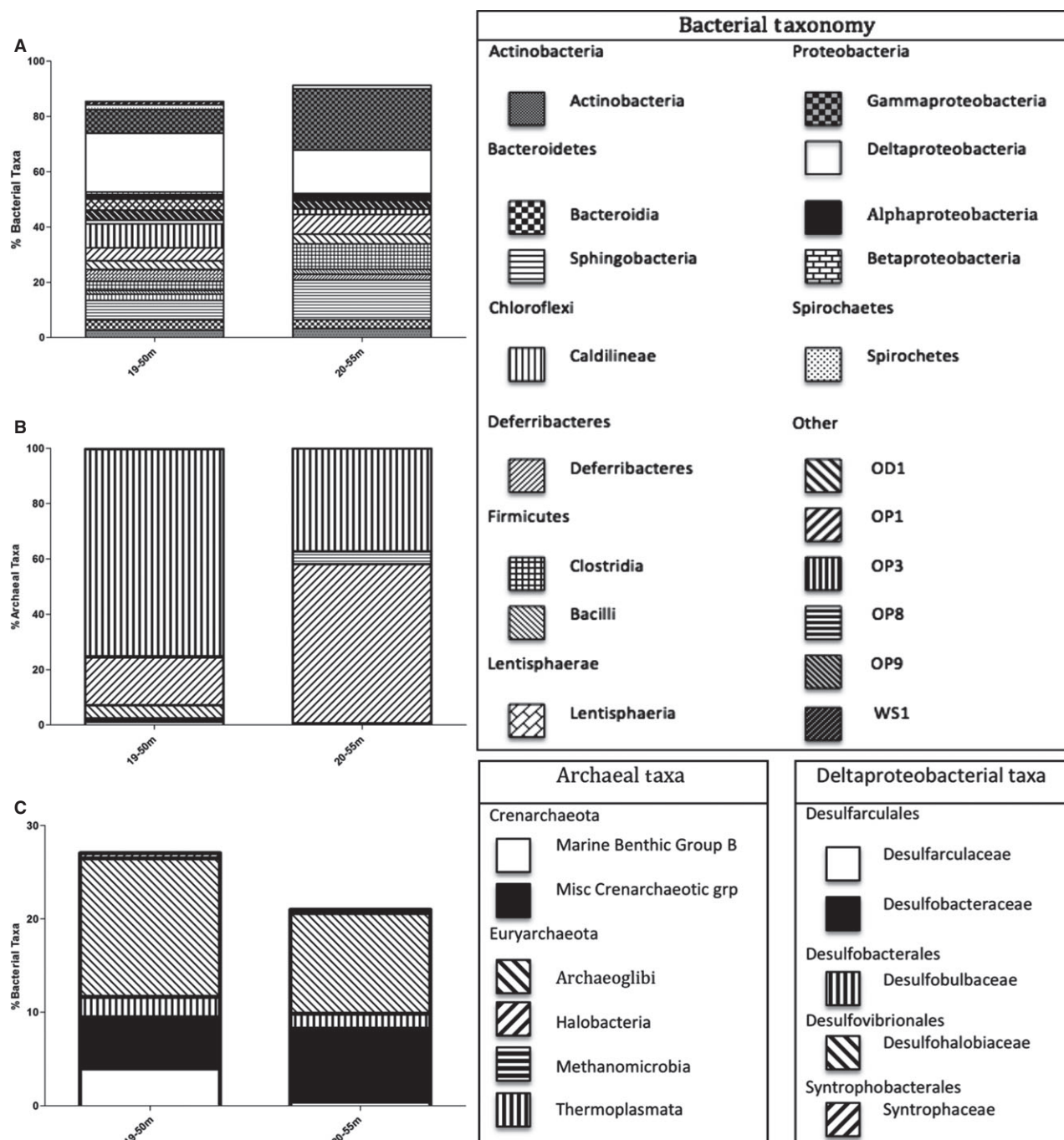


Fig. 5 (A) Bacterial taxon as a percentage of total bacterial taxon. Taxons are resolved at class level. (B) Archaeal taxon shown as a percentage of total archaeal taxon. Taxons are resolved at class level (C) Deltaproteobacterial taxon as a percentage of total bacterial taxon. Taxons are resolved at family level.

some of the carbon of the DS solution was lost while penetrating into the aquifer while another source was added. These two samples with the missing DIC emphasize the low $\delta^{13}\text{C}$ of the substrate involved, as precipitation of carbonate minerals is expected to enrich the residual DIC with the heavy isotopes (+2.5‰, Mook, 1980). However, in the last two samples (EG20/55 and EG22/25

sites), if the excess DIC was derived solely from AOM, the $\delta^{13}\text{C}_{\text{DIC}}$ would have been lighter than that measured. Thus, it seems that the carbon in these samples originated from a combination of both methane and organic matter oxidation.

The source of the methane could be a deep thermogenic one, as suggested for the hydrocarbon gases in the DS rift

Table 3 Estimation of the DIC source (organic matter oxidation (OM) or methane oxidation) in DS circulating groundwater

Sample	Measured DIC (mM)	Initial DS DIC (mM)	Surplus DIC (mM)	Initial DS $\delta^{13}\text{C}_{\text{DIC}}$ (‰)	Expected $\delta^{13}\text{C}_{\text{DIC}}$ following OM oxidation (‰)	Expected $\delta^{13}\text{C}_{\text{DIC}}$ following CH_4 oxidation (‰)	Measured $\delta^{13}\text{C}_{\text{DIC}}$ (‰)
EG15/19*	0.60	0.98	-0.38	2.8	-	-	-15.4
EG16/11*	0.57	0.98	-0.41	2.8	-	-	-10.2
EG20/55*	1.87	0.98	0.89	2.8	-10.4	-17.6	-17.0
EG22/25*	1.80	0.98	0.82	2.8	-9.9	-16.7	-14.1

*After Avrahamov *et al.* (2010).

(Gvirtzman & Stanislavsky, 2000) or a deep biogenic source. The fact that the $\delta^{13}\text{C}_{\text{CH}_4}$ is not overwhelmingly ^{12}C rich may support the thermogenic source; however, we cannot rule out a biogenic source based on C isotopes alone. Methanogenesis is not likely to occur *in situ* at the depth of the groundwater as evident by the light $\delta^{13}\text{C}_{\text{DIC}}$ values and the presence of sulfate (minimal value of 2 mM), unless some alternative non-competitive substrate such as methanol or methylamine (not measured) is involved (Oremland & Polcin, 1982; Marvin Di Pasquale *et al.*, 1999).

SO_4 and $\delta^{34}\text{S}$

Sulfate concentrations along the groundwater flow path reflect complex and multiple processes. Although the DS salinity is mainly preserved in the circulating DS groundwater, the sulfate concentration is lower in this hypersaline groundwater compared with the DS water (2.9 mM vs. 4 mM, respectively). As the DS water is oversaturated with respect to gypsum ($\Omega_{\text{gyp}} = 1.4$), it is reasonable to assume that gypsum precipitation accounts for some of these decreases. Maximum sulfate removal through precipitation can be determined from the difference in concentration between the expected sulfate due to mixing and sulfate concentration at saturation. Indeed, 5 m inland from the shore, the saturation state for gypsum (Ω_{gyp}) has decreased to between 0.9 and 1.0. As the DS groundwater continues circulating, the Ω_{gyp} drops to 0.6 (80 m from the lake, EG20/55 m), suggesting an additional sink for sulfate or calcium. The additional sink can be determined from the difference between the sulfate concentrations at saturation and the measured concentration. The $\delta^{34}\text{S}_{\text{SO}_4}$ measured in the aqueous sulfate at EG20/55 m is 21.9‰, which is isotopically heavier (^{34}S rich) compared with the original DS brine (15‰), suggesting that ^{32}S was removed from the circulating sulfate. While not definitive, this is very suggestive of microbially mediated sulfate reduction occurring in the aquifer and the subsequent removal of the sulfide as FeS phases.

In the FSI zone (1200–6200 Cl^- mM), the sulfate concentrations are higher (up to 31 mM) compared with the circulated DS groundwater, and sulfate concentrations decrease with increasing salinity (Fig. 3B). Due to the

changes in the lake's water level, these data suggest that the extra sulfate source is gypsum dissolution by subsaturated groundwater within the alluvial aquifer that precipitated from the DS in the past, when lake level was higher (e.g., Neev & Hall, 1979). It should be noted that then at the Holocene period, $\delta^{34}\text{S}_{\text{SO}_4}$ value was close to the present DS value (Gavrieli *et al.*, 2001). The Ω_{gyp} of the groundwater in the FSI zone ranges from 0.7 to 1.0; the $\delta^{34}\text{S}_{\text{SO}_4}$ (18.8–21.4‰) is also enriched in ^{34}S , suggesting bacterial sulfate reduction.

Pre-reaction sulfate concentration

To estimate the extent of bacterial sulfate reduction and evaluate its sulfur isotope fractionation factor, the initial sulfate concentration must be known and the water sources must be traced. According to the end members described in the hydrological background, most of the groundwater in the FSI zone is a mixture of the western brine (represented by EG22/19.7) and the DS water in the east. Therefore, the expected mixing value prior to geochemical reactions can be calculated, as previously demonstrated.

The two end member water bodies are supersaturated or saturated with respect to gypsum ($\Omega_{\text{gy}} = 1.4$ and 1.0, for the DS and the western brine, respectively), but the mixtures measured from the boreholes are not saturated ($\Omega_{\text{gy}} < 1$, Table 1). Although gypsum has low precipitation kinetics in the DS brine, precipitation will be promoted when crystallization seeds are available (Reznik *et al.*, 2009), as expected within the alluvial aquifer, and thus, it is reasonable to assume that gypsum precipitation proceeds before biochemical reaction. According to this, the first depletion in sulfate (Fig. 2B) from the expected mixing values at saturation state would be due to gypsum precipitation, while the second depletion would be due to bacterial sulfate reduction. The sulfate concentrations at saturation ($\Omega_{\text{gy}} = 1$) were calculated with the PhreeqC code (Parkhurst & Appelo, 2007), using the Pitzer database for high ionic strength solutions. Precipitation of gypsum during the mixing process explains some of the change in the sulfate concentrations of the DS circulating groundwater but not the isotopic variations, as sulfur isotope fractionation between dissolved sulfate and the precipitated gypsum is negligible (Worden *et al.*, 1997). As

discussed above, the mixed water at the FSI zone maintains higher sulfate concentrations due to gypsum dissolution in the Holocene alluvial aquifer, where this gypsum has a $\delta^{34}\text{S}_{\text{SO}_4}$ value close to that of the present DS (Gavrieli *et al.*, 2001). Confirmation of this gypsum dissolution hypothesis can also be found in the oxygen isotope composition of the sulfate; oxygen isotope fractionation between sulfate and gypsum is around +3.6‰ (Lu *et al.*, 2001). This is reflected in the heavier $\delta^{18}\text{O}_{\text{SO}_4}$ of the western brine end member ($\delta^{18}\text{O}_{\text{SO}_4} = 18.1\text{‰}$), where sulfate concentrations are higher due to gypsum dissolution compared with $\delta^{18}\text{O}_{\text{SO}_4}$ of the DS -13.6‰ . Therefore, it is reasonable to assume that the main process responsible for this sulfate depletion and sulfur isotopic variations is bacterial sulfate reduction and subsequent sulfide precipitation. Given the above, the predicted sulfate concentrations at $\Omega_{\text{gy}} = 1$ were compared with the measured value to estimate the amount of sulfate that was removed by bacterial sulfate reduction (Fig. 3B).

Apparent net BSR and the environmental conditions

Estimating sulfate reduction rates under aquifer conditions is not trivial. Processes such as advection, dispersion, and adsorption can lower sulfate concentration. However, a rough estimation of apparent net sulfate reduction can be achieved by subtracting measured sulfate values from the initial sulfate concentration. Figure 6 shows the sulfate, sulfur, and oxygen isotope compositions as a function of the apparent BSR reaction progress (pre-reaction value minus the measured value). Both the $\delta^{34}\text{S}_{\text{SO}_4}$ and $\delta^{18}\text{O}_{\text{SO}_4}$ show an increase with the progressive sulfate reduction, as expected from the heavy-isotope enrichment in the residual sulfate.

It is generally accepted that sulfate concentrations do not modify sulfate reduction rates unless the concentration is less than 1 mM, or even 200 μM (Martens & Berner, 1977; Jørgensen, 1981; Boudreau & Westrich, 1984). Most of the groundwater samples considered here contain more than 1 mM sulfate, indicating that sulfate concentration is not a primary controlling factor for sulfur isotope fractionation during sulfate reduction.

Besides sulfate concentrations, the observed differences in the apparent bacterial sulfate reduction between the samples may be attributed to temperature, pressure, and the amount of reactive organic carbon in the sediment and the extent to which it can be metabolized (Boudreau & Westrich, 1984 and references therein). In this study, all the samples are from the shallow aquifer, so temperature and hydrostatic pressure effects are irrelevant.

Previous studies have shown that the amount and reactivity of the organic carbon in sediments are the two most important factors controlling the rate of bacterial sulfate reduction (Goldhaber & Kaplan, 1975; Berner, 1978;

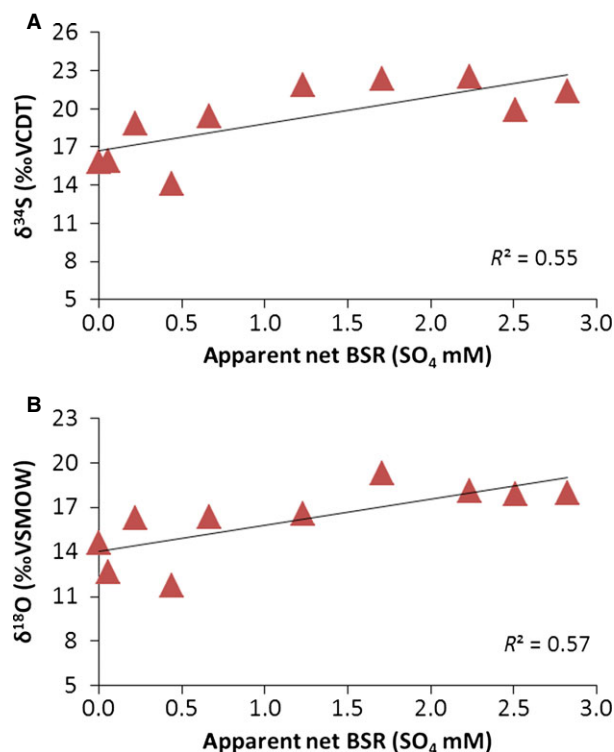


Fig. 6 (A) $^{34}\text{S}_{\text{SO}_4}$ and (B) $^{18}\text{O}_{\text{SO}_4}$ vs. apparent net BSR. The pre-reaction sulfate concentration was determined from the mixing fraction and chemical equilibrium to gypsum as calculated from the Phreeqc model.

Jørgensen, 1981; Westrich, 1983). Of these two variables, the reactivity of the organic carbon is considered to be more important (Westrich, 1983). In this case, the organic carbon available for bacterial sulfate reduction is mostly methane. While it is difficult to oxidize methane, under certain situations, methane can be more available to the sulfate-reducing bacteria than organic matter even though thermodynamically sulfate reduction coupled with methane is less favorable (Sivan *et al.*, 2011 and references therein). The low concentrations of methane suggest that it may limit bacterial sulfate reduction in the groundwater, as indicated by the observed relationship between methane concentration and the apparent net rate bacterial sulfate reduction (Fig. 7A). The increase in the methane concentrations with the flow direction supports an increased net rate of sulfate reduction. We therefore suggest that bacterial sulfate reduction mainly occurs via AOM, although we cannot rule out organoclastic sulfate reduction entirely.

Figure 7B shows an inverse correlation between salinity and AOM ($R^2 = 0.78$). The salinity effect is not clear as there is also a correlation between methane and salinity. However, other studies have shown that hypersaline environments inhibit AOM (Maignien *et al.*, 2013; Joye *et al.*, 2009). In brine sediments of Mercator Marine mud volcanoes, AOM seems to be partially inhibited by hypersaline

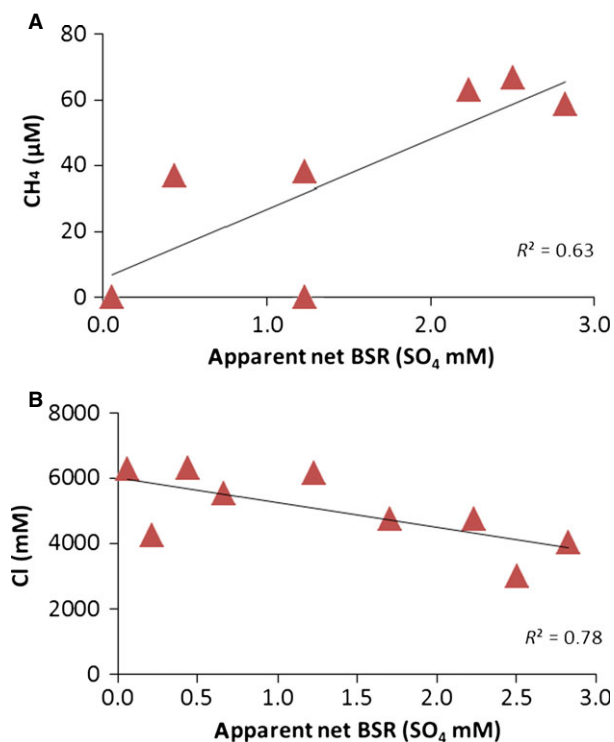


Fig. 7 Methane (A) and Cl⁻ (B) concentrations vs. calculated apparent net BSR. The good correlation between the methane and salinity to the apparent net BSR suggests that methane and salinity might limit BSR coupled with AOM.

conditions (Maignien *et al.*, 2013). AOM appears to be inhibited at high salinity while bacterial sulfate reduction is not inhibited. However, no significant difference in the enrichment factor, ³⁴ε, in hypersaline environments has been demonstrated (Habicht & Canfield, 1997).

Sulfur and oxygen isotope fractionations

The observed inverse relationship between dissolved sulfate and δ³⁴S_{SO₄} values (Fig. 4A) in the hypersaline groundwater fits a Rayleigh distillation of ³²S during sulfate reduction and may be a function of the methane concentrations or other limiting parameters (e.g., dissolved organic carbon concentration). The fractionation factors (α) of sulfur during sulfate reduction can be derived from the Rayleigh equation for a closed system, based on measurements of the isotope ratios and sulfate concentrations (Broecker & Oversby, 1971):

$$R_t/R_0 = (N_t/N_0)^{(\alpha-1)} \quad (4)$$

where R_t and R_0 are the measured isotope ratios of sulfate at time t and at the initiation of sulfate reduction, respectively; α is the fractionation factor for S; (N_t/N_0) is the fraction of sulfate (f) remaining in the groundwater at any

given time. Equation (4) can be rewritten as follows (Aharon, 1985):

$$\Delta\delta = \delta_t - \delta_0 = 10^3 (\alpha - 1) \ln(f) \quad (5)$$

where $\delta_t = \delta^{34}\text{S}$ is the value of the residual sulfate fraction and $\delta_0 = \delta^{34}\text{S}$ is the value of the initial sulfate before microbial sulfate reduction commenced (according to mixing and chemical equilibrium with gypsum). $10^3 \cdot (\alpha - 1)$ is also known as the enrichment factor (ϵ) in permil, which is the preference of ³²S over ³⁴S during bacterial sulfate reduction in the given natural conditions.

Several assumptions related to the origin of the groundwater can be used to constrain a closed system. The trend of increasing δ³⁴S_{SO₄} values in the DS circulating groundwater along the flow path inland, while preserving the salinity in this groundwater, suggests a more advanced reduction stage along the Rayleigh distillation path, provided that the closed systems were maintained and that the initial isotopic compositions were similar. However, in the FSI zone, the two end members of the mixed brines have the same isotopic value (15.9‰ in the DS and 15.8‰ in the western brine). In general, in a closed system, sulfides accumulate. However, it is possible that much of the produced sulfide escaped from the systems through degassing (as hinted at by the low pH of most of the groundwater samples compared to that in the two end members—Table 1) or by its precipitation as metal sulfide. We measured a decrease in ferrous iron concentrations that suggests that metal sulfides may be precipitated along the flow path.

In a plot of Δδ vs. ln(f), the slope represents the enrichment factor ϵ . In practice, the ln(f) member is actually the natural log of the apparent net bacterial sulfate reduction as calculated above and as presented in Fig. 4. The enrichment factor of sulfur (³⁴ε) for the groundwater samples was found to be $17 \pm 3.5\%$ (Fig. 8). Sulfur isotope

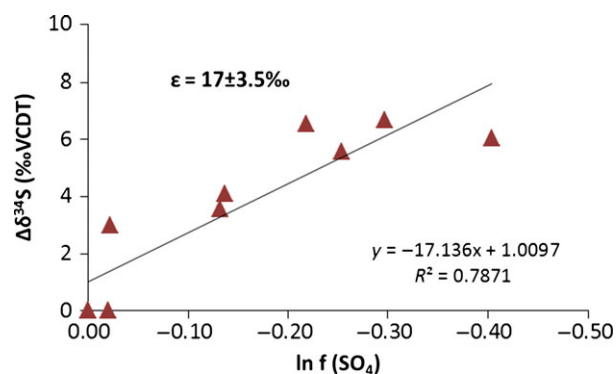


Fig. 8 Sulfur isotope enrichment relative to the pre-reaction value vs. the residual sulfate fraction left in the groundwater after bacterial sulfate reduction (eq. 5). The sulfur isotope enrichment factor (³⁴ε) is the slope of this relationship.

fractionation during bacterial sulfate reduction is a function of various environmental factors. The $^{34}\epsilon$ value calculated here is lower than the upper limit of sulfur isotope fractionations found to be between 0 and 72‰ in the natural environment (Wortmann *et al.*, 2001; Brunner & Bernasconi, 2005; Canfield, 2001; Sim *et al.*, 2011). Small sulfur isotope fractionation ($17 \pm 3.5\%$) may occur under conditions of limited sulfate supply and/or high sulfate reduction rates (e.g., Canfield *et al.*, 2006; Stam *et al.*, 2011; Aharon & Fu, 2000). Given that the sulfate concentrations are high (as discussed above), we suggest that the small sulfur isotope fractionation may result from a high rate of bacterial sulfate reduction, which involves less re-oxidation of sulfur intermediates (Rees, 1973), as has also been concluded from both experimental data and theoretical work (e.g., Harrison & Thode, 1958; Kaplan & Rittenberg, 1964; Rees, 1973; Canfield *et al.*, 2006; Brunner & Bernasconi, 2005; Sim *et al.*, 2011). To better understand the effect of the substrate and salinity on the fractionation factor, Table 4 presents sulfur isotope fractionation data from different locations classified by their reaction type (organoclastic sulfate reduction vs. sulfate reduction by AOM) and salinity conditions (hypersaline or seawater). As several factors affect bacterial sulfate reduction, a reliable comparison between different sites is difficult and should be taken with caution.

Bacterial sulfate reduction has been documented in hypersaline water of organic rich sediments in Solar Lake in Egypt with a salinity range similar to that of the DS aquifer. In that case, the reported $^{34}\epsilon$ was $\sim 20\%$ (Habicht & Canfield, 1997). In cold seeps in the Gulf of Mexico, the sulfur isotope fractionation factor for bacterial sulfate reduction was 18‰ (Aharon & Fu, 2000) compared with 8.6‰ for bacterial sulfate reduction coupled with AOM at the same site.

The low $^{34}\epsilon$ of the AOM in hypersaline environments compares with the $^{34}\epsilon$ of bacterial sulfate reduction that

may be controlled by the electron donor. As the molecule of methane is smaller and considerably simpler than that of refractory crude oil, some micro-organisms prefer methane over more complex organic matter (Aharon & Fu, 2000), even though thermodynamically it is less energetically favorable as an electron donor (Devol & Ahmed, 1981; Aharon & Fu, 2000). However, higher sulfate reduction rates at the methane-rich site may result from the higher methane availability, making it favorable over the less abundant organic matter. One of these two reasons could explain the current low $^{34}\epsilon$ compared with Gavrieli *et al.*'s (2001) results, which calculated a higher sulfur isotope fractionation factor (30‰).

Besides sulfur isotopes, the oxygen isotopic composition of the residual sulfate contributes valuable information for understanding patterns and regulation of bacterial sulfate reduction (e.g., Fritz *et al.*, 1989; Böttcher *et al.*, 1998; Brunner *et al.*, 2005; Wortmann *et al.*, 2007; Turchyn *et al.*, 2006; Antler *et al.*, 2013). The partitioning of oxygen isotopes in the residual sulfate during bacterial sulfate reduction remains controversial. In the recent literature, two different mechanisms are discussed. The first hypothesis suggests the dominance of a kinetic enrichment of the heavy oxygen isotope in the residual sulfate over the preferential reduction of ^{16}O -bearing sulfate (e.g., Mizutani & Rafter, 1969; Aharon & Fu, 2003; Mandernack *et al.*, 2003). On the other hand, the second hypothesis favors the idea of an isotopic equilibration of the oxygen in the sulfate with ambient water. However, the timescale for abiotic oxygen isotope exchange between water and sulfate is very slow (20–60 million years; Lloyd, 1968; Chiba & Sakai, 1985), leading to the conclusion that oxygen isotope equilibrium is achieved via sulfur compounds generated intracellularly as intermediates during bacterial sulfate reduction (e.g., Mizutani & Rafter, 1973; Fritz *et al.*, 1989; Brunner *et al.*, 2005; Wortmann *et al.*, 2007). According to this, while the sulfur isotope composition

Table 4 Sulfur isotope fractionations by reaction type and salinity conditions in this study and previous studies

Location	Sediment Type	Isotope Fractionation Enrichment Factor, $^{34}\epsilon$ (‰)	References
Sulfate reduction coupled with anaerobic organic matter oxidation			
Hypersaline condition			
Solar Lake, Egypt	Microbial mats	20	(1)
Mono Lake, California	Basaltic sediment	5–21, mean value 12	(2)
Flow-through reactor	Brackish estuarine sediments, 20 °C	Mean value 17	(3)
Sea water salinity			
Gulf of Mexico	Oil seeps	18	(4)
Sulfate reduction coupled with anaerobic methane oxidation			
Seawater salinity			
Gulf of Mexico	Gas seeps	8.6	(4)
Hypersaline condition			
DS basin	Alluvial sediment	17 ± 3.5	(5)

(1) Habicht & Canfield, 1997; (2) Stam *et al.* (2010); (3) Stam *et al.* (2011); (4) Aharon & Fu, 2000; (5) this study.

would increase during bacterial sulfate reduction, the oxygen value would be expected to be concave toward the equilibrium value. However, both isotopes respond to changes in the intermediate steps—fluxes and isotope fractionation (Brunner *et al.*, 2005, 2012; Antler *et al.*, 2013). Therefore, a plot of $\delta^{18}\text{O}_{\text{SO}_4}$ vs. $\delta^{34}\text{S}_{\text{SO}_4}$ can be useful for understanding the dynamics of the intracellular reactions during bacterial sulfate reduction (Brunner *et al.*, 2005, 2012; Antler *et al.*, 2013).

Figure 9 shows a linear correlation between $\delta^{18}\text{O}_{\text{SO}_4}$ and $\delta^{34}\text{S}_{\text{SO}_4}$ in the DS aquifer ($R^2 = 0.86$). The moderate slope (0.76) indicates that the sulfur isotopes increase more rapidly relative to the oxygen isotopes. Figure 9 also demonstrates the expected isotopic ‘plateau’ for the oxygen isotope where there is full oxygen isotope equilibrium between the ambient water and sulfate. Previous studies found that the $\delta^{18}\text{O}_{\text{SO}_4}$ equilibrium value with water is between 22 and 30‰ higher than the ambient $\delta^{18}\text{O}$ water (Fritz *et al.*, 1989; Böttcher *et al.*, 1998; Turchyn *et al.*, 2006; Wortmann *et al.*, 2007; Aller *et al.*, 2010; Antler *et al.*, 2013). According to the $\delta^{18}\text{O}_{\text{H}_2\text{O}}$ of the groundwater which ranged between -3.3‰ and 3.9‰, the oxygen isotopic equilibrium would be expected to be +25‰–+35‰ (Fig. 9). Theoretically, the linear correlation between $\delta^{18}\text{O}_{\text{SO}_4}$ vs. $\delta^{34}\text{S}_{\text{SO}_4}$ and the fact that $\delta^{18}\text{O}_{\text{SO}_4}$ is still not at equilibrium suggest that the kinetic isotope effects control both sulfur and oxygen isotope evolution during bacterial sulfate reduction. In traditional bacterial sulfate reduction, lower rates of sulfate reduction with more re-oxidation of sulfate intermediates lead to an equilibrium curve with $\delta^{18}\text{O}_{\text{SO}_4}$ value of sulfite exchange with water and oxidation. However, the linear relationship can also be explained as the tangent of a concaved shape toward equilibrium (Brunner *et al.*, 2005; Antler *et al.*, 2013), and therefore, oxygen isotopic equilibration between sulfate and water cannot be entirely ruled out.

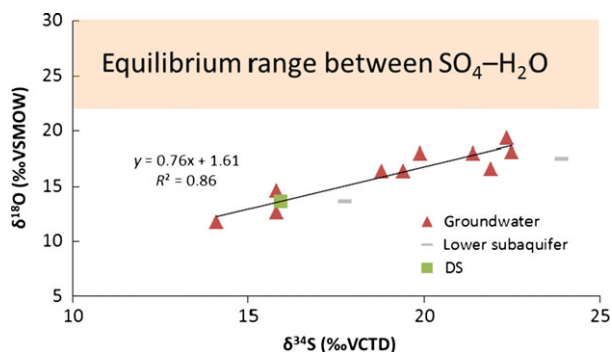


Fig. 9 $\delta^{18}\text{O}_{\text{SO}_4}$ vs. $\delta^{34}\text{S}_{\text{SO}_4}$ sulfate data in the groundwater samples display a positive relation. The predicted range of equilibrium isotope fractionations between SO_4^{2-} and H_2O are indicated by the pink area (estimated from Fritz *et al.*, 1989; Brunner *et al.*, 2005; Turchyn *et al.*, 2006; Wortmann *et al.*, 2007; Aller *et al.*, 2010).

The slope of $\delta^{18}\text{O}_{\text{SO}_4}$ vs. $\delta^{34}\text{S}_{\text{SO}_4}$ has been related to the rate of bacterial sulfate reduction (Böttcher *et al.*, 1998; Antler *et al.*, 2013). The slope of $\delta^{18}\text{O}_{\text{SO}_4}$ vs. $\delta^{34}\text{S}_{\text{SO}_4}$ found in this study, 0.76 (Fig. 9), is close to the range reported by Aharon & Fu (2000) for sulfate-driven AOM in the high salinity cold seeps from the Gulf of Mexico (0.3–0.7). In their work, the rate of bacterial sulfate reduction varied over almost two orders of magnitude ($\sim 5 \times 10^{-4}$ to $\sim 2 \times 10^{-6}$ mol cm^{-3} year $^{-1}$). Although these rates were not directly measured but were modeled from the pore fluid sulfate concentration profile, they are much higher than those that have been observed in deep-sea sediments (up to 7 orders of magnitude higher—Turchyn *et al.*, 2006; Wortmann *et al.*, 2007; Antler *et al.*, 2013). Therefore, even though we were not able to calculate the rate of bacterial sulfate reduction directly in this study due to the poorly constrained physical properties of our system, we suggest, based on the slope of $\delta^{18}\text{O}_{\text{SO}_4}$ vs. $\delta^{34}\text{S}_{\text{SO}_4}$, that the rate of bacterial sulfate reduction is comparable to that observed at gas and oil seeps (Aharon & Fu, 2000, 2003; Rubin-Blum *et al.*, 2014) or estuaries (Antler *et al.*, 2013), supporting our link between bacterial sulfate reduction and AOM. In addition, it has recently been shown that during the AOM in seeps or estuaries, a linear correlation between $\delta^{18}\text{O}_{\text{SO}_4}$ vs. $\delta^{34}\text{S}_{\text{SO}_4}$ is observed (Antler *et al.*, 2014).

Microbial taxon

Overall, the microbial community supports the geochemical evidence, suggesting that the aquifer supports coupled AOM and sulfate reduction. The bacterial community in particular is indicative of bacterial sulfate reduction and association with ANME in general (Knittel & Boetius, 2009; Rabus *et al.*, 2013). Desulfobacteriaceae sequences are commonly observed in libraries sequenced from hypersaline environments (La Cono *et al.*, 2011), and while strains of this class have been observed to reduce sulfate in culture (Jakobsen *et al.*, 2006), none have been observed to be a part of an ANME-SRB consortium. The abundant taxon Desulfobacteraceae has been shown to be associated with ANME previously (Pentthaler *et al.*, 2008).

Despite the high relative abundance of Euryarchaeota, Methanomicrobia was the only taxon containing marine ANME groups to be observed at either site (Fig. 5B, 0.37% EG19, 4.58% EG20). This result is less surprising in light of previous studies showing hypersaline sites to be sources of previously unidentified diversity among methane-oxidizing microbes (Scholten *et al.*, 2005). The Euryarchaeota Thermoplasma is a taxon that might also be involved with methane oxidation at this site. Included in this group is marine benthic group B or deep-sea archaeal group. This taxon has been implicated in AOM previously,

as it is frequently identified in methane-hydrate-bearing sediments (Inagaki *et al.*, 2006b; Roalkvam *et al.*, 2011).

SUMMARY

The anoxic part of the FSI zone in the DS aquifer was used to explore sulfur and oxygen isotope systematics of sulfate in hypersaline groundwater (up to 6300 mM) due to sulfate-driven AOM. Correlation between $\delta^{34}\text{S}_{\text{SO}_4}$ and sulfate depletion indicated bacterial sulfate reduction. The anaerobic conditions and the isotope mass balances suggest that the observed decrease in $\delta^{13}\text{C}_{\text{DIC}}$ is mainly a result of methane oxidation (AOM) through this BSR. The microbial taxon observed support the geochemical evidence. In particular, the bacterial community is indicative of bacterial sulfate reduction and association with ANME. The apparent net bacterial sulfate reduction rate has been calculated. The extent of sulfate removal by reduction is correlated with the salinity and methane concentrations, suggesting that the two major factors controlling the variable reduction in the DS area are the salinity and methane availability. According to the Rayleigh equation, the sulfur isotope fractionation during bacterial sulfate reduction in the FSI zone is $17 \pm 3.5\text{‰}$, considerably lower than that found in the DS in the past ($^{34}\epsilon = 30\text{‰}$) for bacterial sulfate reduction that is not associated with AOM. This low value ($17 \pm 3.5\text{‰}$) may indicate a higher oxidation rate of methane compared with that of organic matter as suggested in previous reports. In this study, the plot of $\delta^{18}\text{O}_{\text{SO}_4}$ vs. $\delta^{34}\text{S}_{\text{SO}_4}$ shows a linear trend without reaching the equilibrium value between the ambient water and sulfate. This could be a result of a kinetic isotope effect, although the equilibrium effect cannot be entirely ruled out. In addition, the slope value of 0.76 suggests a high rate of bacterial sulfate reduction. Improvement of the parameters controlling oxygen isotope ratios in the future by defining precisely the oxygen isotope fractionation during bacterial sulfate reduction likewise increasing identification of methane-oxidizing microbes diversity in hypersaline environments could improve our understanding of the AOM reaction in the DS area.

ACKNOWLEDGMENTS

We thank the two anonymous reviewers for their thorough and helpful reviews, and M. Stiller for her comments. We thank Dr Y. Rosenberg from Ben Gurion University for the help with the sulfate analyses. Major ion analyses were carried out in the laboratory of the Geological Survey of Israel with the help of D. Stiber and O. Yoffe. Field work was performed with the help of H. Hemo and H. Lutsky from the Geological Survey of Israel. We thank also J. Battles, H. Morrison, and M. Sogin for assistance with sequencing. This research was supported by the Israeli Ministry of

Energy & Water Resources and the US National Science Foundation award number—EF-0801741.

REFERENCES

- Aharon P (1985) Carbon isotope record of late Quaternary coral reefs: possible index of sea surface paleoproductivity. *Geophysical Monograph Series* **32**, 343–355.
- Aharon P, Fu B (2000) Microbial sulfate reduction rates and sulfur and oxygen isotope fractionations at oil and gas seeps in deepwater Gulf of Mexico. *Geochimica et Cosmochimica Acta* **64**, 233–246.
- Aharon P, Fu B (2003) Sulfur and oxygen isotopes of coeval sulfates sulfide in pore fluids of cold seep sediments with sharp redox gradients. *Chemical Geology* **195**, 201–218.
- Alain K, Holler T, Musat F, Elvert M, Treude T, Krüger M (2006) Microbiological investigation of methane- and hydrocarbon-discharging mud volcanoes in the Carpathian Mountains, Romania. *Environmental Microbiology* **8**, 574–590.
- Aller RC, Madrid V, Chistoserdov A, Aller JY, Heilbrun C (2010) Unsteady diagenetic processes and sulfur biogeochemistry in tropical deltaic muds: Implications for oceanic isotope cycles and the sedimentary record. *Geochimica et Cosmochimica Acta* **74**, 4671–4692.
- Alperin MJ, Hoehler TM (2009) Anaerobic methane oxidation by archaea/sulfate-reducing bacteria aggregates: 1. Thermodynamic and physical constraints. *American Journal of Science* **309**, 869–957.
- Alperin MJ, Reeburgh WS, Whiticar MJ (1988) Carbon and hydrogen isotope fractionation resulting from anaerobic methane oxidation. *Global Biogeochemical Cycles* **2**, 279–288.
- Altschul SF, Gish W, Miller W, Myers EW, Lipman DJ (1990) Basic local alignment search tool. *Journal of Molecular Biology* **215**, 403–410.
- Anati AD, Shasha S (1989) Dead Sea surface level changes. *Israel Journal of Earth Sciences* **16**, 181–196.
- Antler G, Turchyn AV, Rennie V, Herut B, Sivan O (2013) Coupled sulfur and oxygen isotope insight into bacterial sulfate reduction in the natural environment. *Geochimica et Cosmochimica Acta* **118**, 98–117.
- Antler G, Turchyn AV, Herut B, Davies A, Rennie VC, Sivan O (2014) Sulfur and oxygen isotope tracing of sulfate driven anaerobic methane oxidation in estuarine sediments. *Estuarine, Coastal and Shelf Science* **142**, 4–11.
- APHA, American Public Health Association, American Water Works Association and Pollution Control Federation (1985) *Standard Methods for the Examination of Water and Wastewater*, 16th edn. APHA, AWWA, WPCF, Washington, DC, pp. 1268.
- Arad A, Michaeli A (1967) Hydrogeological investigations in the western catchment of the Dead Sea. *Israel Journal of Earth Sciences* **16**, 181–196.
- Aврахамов N, Yechieli Y, Lazar B, Lewenberg O, Boaretto E, Sivan O (2010) Characterization and dating of saline groundwater in the Dead Sea area. *Radiocarbon* **52**, 1123–1140.
- Barkan E, Luz B, Lazar B (2001) Dynamics of the carbon dioxide system in the Dead Sea. *Geochimica et Cosmochimica Acta* **65**, 355–368.
- Basen M, Krüger M, Miluckal J, Kuever J, Kahnt J, Grundmann I O, Meyerdierks A, Widdel F, Shima S (2011) Bacterial enzymes for dissimilatory sulfate reduction in a marine microbial mat

- (Black Sea) mediating anaerobic oxidation of methane. *Environmental Microbiology* **13**, 1370–1379.
- Berner RA (1978) Sulfate reduction and the rate of decomposition of marine sediments. *Earth and Planetary Science Letters* **37**, 492–498.
- Boetius A, Ravensschlag K, Schubert CJ, Rickert D, Widdel F, Gieseke A, Amann R, Jørgensen BB, Witte U, Pfannkuche O (2000) A marine microbial consortium apparently mediating anaerobic oxidation of methane. *Nature* **407**, 623–626.
- Böttcher ME, Brumsack HJ, de Lange GJ (1998) Sulfate reduction and related stable isotope (^{34}S , ^{18}O) variations in interstitial waters from the eastern Mediterranean. In *Proceedings of the Ocean Drilling Program - Scientific Results* (eds Robertson AHF, Ermeis KC, Richter C, Camerlenghi A) 160: Ocean Drilling Program, College Station, TX, pp. 365–373.
- Boudreau BP, Westrich JT (1984) The dependence of bacterial sulfate reduction on sulfate concentration in marine sediments. *Geochimica et Cosmochimica Acta* **48**, 2503–2516.
- Brandt KK, Vester F, Jensen AN, Ingvorsen K (2001) Sulfate reduction dynamics and enumeration of sulfate-reducing bacteria in hypersaline sediments of the Great Salt Lake (Utah, USA). *Microbial Ecology* **41**, 1–11.
- Brazelton WJ, Schrenk MO, Kelley DS, Baross JA (2006) Methane- and sulfur-metabolizing microbial communities dominate the Lost City hydrothermal field ecosystem. *Applied and Environmental Microbiology* **72**, 6257–6270.
- Broecker WS, Oversby VM (1971) *Chemical Equilibria in the Earth*. McGraw-Hill, New York, p. 318.
- Brunner B, Bernasconi SM (2005) A revised isotope fractionation model for dissimilatory sulfate reduction in sulfate reducing bacteria. *Geochimica et Cosmochimica Acta* **69**, 4759–4771.
- Brunner B, Bernasconi SM, Kleikemper J, Schroth MH (2005) A model for oxygen and sulfur isotope fractionation in sulfate during bacterial sulfate reduction processes. *Geochimica et Cosmochimica Acta* **69**, 4773–4785.
- Brunner B, Einsiedl F, Arnold GL, Müller I, Templer S, Bernasconi S (2012) The reversibility of dissimilatory sulphate reduction and the cell-internal multistep reduction of sulphite to sulphide: insights from the oxygen isotope composition of sulphate. *Isotopes in Environmental & Health Studies* **48**, 33–54.
- Canfield DE (2001) Isotope fractionation by natural populations of sulfate reducing bacteria. *Geochimica et Cosmochimica Acta* **65**, 1117–1124.
- Canfield DE, Des Marais DJ (1991) Aerobic sulfate reduction in microbial mats. *Science* **251**, 1471–1473.
- Canfield DE, Olesen CA, Cox RP (2006) Temperature and its control of isotope fractionation by a sulfate-reducing bacterium. *Geochimica et Cosmochimica Acta* **70**, 548–561.
- Caporaso JG, Kuczynski J, Stombaugh J, Bittinger K, Bushman FD, Costello EK, Fierer N, Pena AG, Goodrich JK, Gordon JL, Huttley GA, Kelley ST, Knights D, Koenig JE, Ley RE, Lozupone CA, McDonald D, Muegge BD, Pirrung M, Reeder J, Sevinsky JR, Tumbaugh PJ, Walters WA, Widmann J, Yatsunenko T, Zaneveld J, Knight R (2010) QIIME allows analysis of high-throughput community sequencing data. *Nature Methods* **7**, 335–336.
- Chiba H, Sakai H (1985) Oxygen isotope exchange rate between dissolved sulfate and water at hydrothermal temperatures. *Geochimica et Cosmochimica Acta* **49**, 993–1000.
- Devol AH, Ahmed SI (1981) Are high rates of sulfate reduction associated with anaerobic oxidation of methane? *Nature* **291**, 407–408.
- Edgar RC (2004) MUSCLE: multiple sequence alignment with high accuracy and high throughput. *Nucleic Acids Research* **32**, 1792–1797.
- Edgar RC (2010) Search and clustering orders of magnitude faster than BLAST. *Bioinformatics* **26**, 2460–2461.
- Edgar RC, Haas BJ, Clemente JC, Quince C, Knight R (2011) UCHIME improves sensitivity and speed of chimera detection. *Bioinformatics* **27**, 2194–2200.
- Eller G, Kanel LK, Krüger M (2005) Co-occurrence of aerobic and anaerobic methane oxidation in the water column of Lake Plusssee. *Applied and Environmental Microbiology* **71**, 8925–8928.
- Fritz P, Basharmal GM, Drimmie RJ, Ibsen J, Qureshi RM (1989) Oxygen isotope exchange between sulfate and water during bacterial reduction of sulfate. *Chemical Geology* **79**, 99–105.
- Froelich PN, Klinkhammer GP, Bender ML, Luedtke GR, Heath GR, Cullen D, Dauphin P, Hammond D, Hartman B, Maynard V (1979) Early oxidation of organic matter in pelagic sediments of the eastern equatorial Atlantic: suboxic diagenesis. *Geochimica et Cosmochimica Acta* **43**, 1075–1090.
- Gavrieli I (1997) Halite Deposition from the Dead Sea: 1960–1993. In: *The Dead Sea – the Lake and Its Setting* (eds Niemi TM, Ben-Avraham Z, Gat JR). Oxford University Press, New York, Oxford, pp. 161–170.
- Gavrieli I, Yechieli Y, Halicz L, Spiro B, Bein A, Efron D (2001) The sulfur system in anoxic subsurface brines and its implication in brine evolutionary pathways: the Ca-chloride brines in the Dead Sea area. *Earth and Planetary Science Letters* **186**, 199–213.
- Goldhaber MB, Kaplan IR (1975) Controls and consequences of sulfate reduction in recent marine sediments. *Soil Science* **119**, 42–55.
- Grossman EL, Cifuentes LA, Cozzarelli IM (2002) Anaerobic methane oxidation in a landfill-leachate plume. *Environmental Science and Technology* **36**, 2436–2442.
- Gvirtzman H, Stanislavsky E (2000) Paleohydrology of hydrocarbon maturation, migration and accumulation in the Dead Sea Rift. *Basin Research* **12**, 79–93.
- Habicht KS, Canfield DE (1997) Sulfur isotope fractionation during bacterial sulfate reduction in organic-rich sediments. *Geochimica et Cosmochimica Acta* **34**, 5351–5356.
- Harrison A, Thode H (1958) Mechanism of the bacterial reduction of sulphate from isotope fractionation studies. *Transactions of the Faraday Society* **54**, 84–92.
- Hoehler TM, Alperin MJ, Albert DB, Martens CS (1994) Field and laboratory studies of methane oxidation in an anoxic marine sediment—Evidence for a methanogen-sulfate reducer consortium. *Global Biogeochemical Cycles* **8**, 451–463.
- Holler T, Widdel F, Knittel K, Amann R, Kellermann MY, Hinrichs KU, Teske A, Boetius A, Wegener G (2011) Thermophilic anaerobic oxidation of methane by marine microbial consortia. *The ISME Journal* **5**, 1946–1956.
- Huse SM, Huber JA, Morrison HG, Sogin ML, Mark Welch D (2007) Accuracy and quality of massively parallel DNA pyrosequencing. *Genome Biology* **8**, R143.
- Inagaki F, Kuypers MMM, Tsunogai U, Ishibashi J, Nakamura K (2006a) Microbial community in a sediment-hosted CO₂ lake of the southern Okinawa Trough hydrothermal system. *Proceedings of the National Academy of Sciences* **103**, 14164–14169.
- Inagaki F, Nunoura T, Nakagawa S, Teske A, Lever M, Lauer A, Suzuki M, Takai K, Delwiche M, Colwell FS (2006b) Biogeographical distribution and diversity of microbes in methane hydrate-bearing deep marine sediments on the Pacific

- Ocean Margin. *Proceedings of the National Academy of Sciences of the United States of America* **103**, 2815–2820.
- Jakobsen TF, Kjeldsen KU, Ingvorsen K (2006) *Desulfohalobium utahense* sp. nov., a moderately halophilic, sulfate-reducing bacterium isolated from Great Salt Lake. *International journal of systematic and evolutionary microbiology* **56**, 2063–2069.
- Jørgensen BB (1983) The microbial sulfur cycle. In: *Microbial Geochemistry* (ed. Krumbein WE). Blackwell, Oxford, pp. 91–124.
- Joye SB, Samarkin VA, Bowles MW, Carini SA, Crespo-Medina M, Madigan MT (2009) Patterns and controls on anaerobic oxidation of methane in extreme environments of varying salinity. In: *Goldschmidt Conference Abstracts 2009*.
- Kaplan IR, Rittenberg SC (1964) Microbiological fractionation of sulphur isotopes. *Journal of General Microbiology* **34**, 195–212.
- Kasten S, Jørgensen BB (2000) Sulfate Reduction in Marine Sediments. In: *Marine Geochemistry* (eds Schulz HD, Zabel M). Springer, Berlin, pp. 263–281.
- Kiro Y (2007) The effect of the Dead Sea level drop in the last fifty years on the groundwater system in the alluvial aquifer and its vicinity. MSc thesis, The Hebrew University of Jerusalem (in Hebrew).
- Kiro Y, Yechieli Y, Lyakhovskiy V, Shalev E, Starinsky A (2008) Time response of the water table and saltwater transition zone to a base level drop. *Water Resources Research* **44**, W12442.
- Knittel K, Boetius A (2009) Anaerobic oxidation of methane: progress with an unknown process. *Annual Review of Microbiology* **63**, 311–334.
- La Cono V, Smedile F, Bortoluzzi G, Arcadi E, Maimone G, Messina E, Borghini M, Oliveri E, Mazzola S, L'Haridon S (2011) Unveiling microbial life in new deep-sea hypersaline Lake Thetis. Part I: prokaryotes and environmental settings. *Environmental Microbiology* **13**, 2250–2268.
- Lensky NG, Dvorkin YL, Lyakhovskiy V, Gertman I, Gavrieli I (2005) Water, salt, and energy balances of the Dead Sea. *Water Resources Research* **41**, W12418.
- Lewenberg O (2005) The hydrogeology and geochemistry of groundwater in the alluvial fan of Wadi Arugot, En Gedi reservation, MSc thesis. The Hebrew University of Jerusalem (in Hebrew).
- Lloyd RM (1968) Oxygen isotope behavior in sulfate–water system. *Journal of Geophysical Research* **73**, 6099–6110.
- Lloyd KG, Lapham L, Teske A (2006) An anaerobic methane-oxidizing community of ANME-1b archaea in hypersaline Gulf of Mexico sediments. *Applied and Environmental Microbiology* **72**, 7218–7230.
- Lu FH, Meyers WJ, Schoonen MA (2001) S and O (SO₄) isotopes, simultaneous modeling, and environmental significance of the Nijar Messinian gypsum, Spain. *Geochimica et Cosmochimica Acta* **65**, 3081–3092.
- Maignien L, Parkes RJ, Cragg B, Niemann H, Knittel K, Coulon S, Akhmetzhanov A, Boon N (2013) Anaerobic oxidation of methane in hypersaline cold seep sediments *FEMS Microbiology Ecology* **83**, 214–231.
- Mandernack KW, Krouse HR, Skei JM (2003) A stable sulfur and oxygen isotopic investigation of sulfur cycling in an anoxic marine basin, Framvaren Fjord, Norway. *Chemical Geology* **195**, 181–200.
- Martens CS, Berner RA (1977) Interstitial water chemistry of anoxic Long Island Sound sediments: I. Dissolved gases. *Limnology and Oceanography* **22**, 10–25.
- Martens CS, Albert DB, Alperin MJ (1999) Stable isotope tracing of anaerobic methane oxidation in the gassy sediments of Eckernförde Bay, German Baltic Sea. *American Journal of Science* **299**, 589–610.
- Marvin Di Pasquale M, Oren A, Cohen Y, Oremland RS (1999) Radiotracer studies of bacterial methanogenesis in sediments from the Dead Sea and Solar Lake (Sinai). In *Microbiology and Biogeochemistry of Hypersaline Environments*. (ed Oren A). CRC Press, Boca Raton, FL, pp. 149–160.
- Milucka J, Ferdelman TG, Polerecky L, Franzke D, Wegener G, Schmid M, Lieberwirth I, Wagner M, Widdel F, Kuypers MMM (2012) Zero-valent sulphur is a key intermediate in marine methane oxidation. *Nature* **491**, 541–546.
- Mitzutani Y, Rafter TA (1969) Oxygen isotope composition of sulphates: 3. Oxygen isotope fractionation in the bisulphate ion–water system. *New Zealand Journal of Science* **12**, 54–59.
- Mizutani Y, Rafter TA (1973) Isotopic behaviour of sulphate oxygen in the bacterial reduction of sulphate. *Geochemical Journal* **6**, 183–191.
- Mook WG (1980) Carbon-14 in hydrogeological studies. In: *Handbook of Environmental Isotope Geochemistry*. Volume 1, Chapter 9. (eds Fritz P, Fontes JC), Elsevier, Amsterdam, pp. 49–74.
- Murray AE, Kenig F, Fritsen CH, McKay CP, Cawley KM, Edwards R, Kuhna E, McKnight DM, Ostromf NE, Penga V, Ponceg A, Prischuh JC, Samarkini V, Townsendj AT, Wagha P, Youngk SA, Yung PT, Doranb PT (2012) Microbial life at –13°C in the brine of an ice-sealed Antarctic lake. *PNAS* **109**, 20626–20631.
- Neev D, Emery KO (1967) *The Dead Sea – Depositional processes and environments of evaporates*. Ministry of Development – Geological Survey of Israel, Jerusalem, 147 p.
- Neev D, Hall JK (1979) Geophysical investigations in the Dead Sea. *Sedimentary Geology* **23**, 209–238.
- Niewöhner C, Hensen C, Kasten S, Zabel M, Schulz HD (1998) Deep sulfate reduction completely mediated by anaerobic methane oxidation in sediments of the upwelling area off Namibia. *Geochimica et Cosmochimica Acta* **62**, 455–464.
- Nishri A, Ben-Yaakov S (1990) Solubility of oxygen in the Dead Sea brine. *Hydrobiologia* **197**, 99–104.
- Nissenbaum A, Kaplan IR (1976) Sulfur and carbon isotopic evidence for biogeochemical processes in the Dead Sea ecosystem. In: *Environmental Biochemistry*, Vol 1 (ed. Nriagu JO), Ann Arbor Science Publishers, Ann Arbor, pp. 309–325.
- Orcutt B, Boetius A, Elvert M, Samarkin V, Joye SB (2005) Molecular biogeochemistry of sulfate reduction, methanogenesis and the anaerobic oxidation of methane at Gulf of Mexico cold seeps. *Geochimica et Cosmochimica Acta* **69**, 4267–4281.
- Oremland RS, Polcin S (1982) Methanogenesis and sulfate reduction: competitive and noncompetitive substrates in estuarine sediments. *Applied and Environmental Microbiology* **44**, 1270–1276.
- Oren A (2011) Thermodynamic limits to microbial life at high salt concentrations. *Environmental Microbiology* **13**, 1908–1923.
- Parkhurst DL, Appelo CAJ (2007) PHREEQC 2.14.3 A computer program for speciation, batch-reaction, one-dimensional transport and inverse geochemical calculation. *Water-Resources Investigation Report 99-4259*. US Geological Survey.
- Pernthaler A, Dekas AE, Brown CT, Goffredi SK, Embaye T, Orphan VJ (2008) Diverse syntrophic partnerships from deep-sea methane vents revealed by direct cell capture and metagenomics. *Proceedings of the National Academy of Sciences* **105**, 7052–7057.
- Porter D, Roychoudhury AN, Cowan D (2007) Dissimilatory sulfate reduction in hypersaline coastal pans: activity across a

- salinity gradient. *Geochimica et Cosmochimica Acta* **71**, 5102–5116.
- Quast C, Pruesse E, Yilmaz P, Gerken J, Schweer T, Yarza P, Peplies J, Glockner FO (2013) The SILVA ribosomal RNA gene database project: improved data processing and web-based tools. *Nucleic Acids Research* **41**(D1), D590–D596.
- Rabus R, Hansen T, Widdel F (2013) Dissimilatory Sulfate- and Sulfur-Reducing Prokaryotes. In *Rosenberg E, DeLong E, Lory S, Stackebrandt E.* (ed Thompson F). *The Prokaryotes*. Springer, Berlin Heidelberg, pp. 309–404.
- Rees CE (1973) A steady-state model for sulphur isotope fractionation in bacterial reduction processes. *Geochimica et Cosmochimica Acta* **37**, 1141–1162.
- Reznik IJ, Gavrieli I, Ganor J (2009) Kinetics of gypsum nucleation and crystal growth from Dead Sea brine. *Geochimica et Cosmochimica Acta* **73**, 6218–6230.
- Reznik I, Gavrieli I, Antler G, Ganor J (2011) Kinetics of gypsum crystal growth from high ionic strength solutions: a case study of Dead Sea – seawater mixtures. *Geochimica et Cosmochimica Acta* **75**, 2187–2199.
- Roalkvam I, Jørgensen SL, Chen Y, Stokke R, Dahle H, Hocking WP, Lanzén A, Hafdason H, Steen IH (2011) New insight into stratification of anaerobic methanotrophs in cold seep sediments. *FEMS Microbiology Ecology* **78**, 233–243.
- Roychoudhury AN, Cowan D, Porter D, Valverde A (2013) Dissimilatory sulphate reduction in hypersaline coastal pans: an integrated microbiological and geochemical study. *Geobiology* **11**, 224–233.
- Rubin-Blum M, Antler G, Turchyn AV, Tsadok R, Goodman-Tchernov BN, Shemesh E, Austin JA, Coleman DF, Makovsky Y, Sivan O, Tchernov D (2014) Hydrocarbon-related microbial processes in the deep sediments of the Eastern Mediterranean Levantine Basin. *FEMS Microbiology Ecology* **87**, 780–796.
- Sambrook J, Russell DW (2001) *Molecular Cloning: A Laboratory Manual*. Cold Spring Harbor Laboratory Press, New York.
- Scholten JCM, Joye SB, Hollibaugh JT, Murrell JC (2005) Molecular Analysis of the Sulfate Reducing and Archaeal Community in a Meromictic Soda Lake (Mono Lake, California) by Targeting 16S rRNA, mcrA, apsA, and dsrAB Genes. *Microbial ecology* **50**, 29–39.
- Segarra KEA, Comerford C, Slaughter J, Joye SB (2013) Impact of electron acceptor availability on the anaerobic oxidation of methane in coastal freshwater and marine sediments. *Geochimica et Cosmochimica Acta* **115**, 15–30.
- Sim MS, Bosak T, Ono S (2011) Large sulfur isotope fractionation does not require disproportionation. *Science* **333**, 74–77.
- Sivan O, Adler M, Pearson A, Gelman F, Bar-Or I, John SG, Eckert W (2011) Geochemical evidence for iron-mediated anaerobic oxidation of methane. *Limnology and Oceanography* **56**, 1536–1544.
- Sivan O, Schrag DP, Murray RW (2007) Rates of methanogenesis and methanotrophy in deep-sea sediments. *Geobiology* **5**, 141–151.
- Sogin ML, Morrison HG, Huber JA, Mark Welch D, Huse SM, Neal PR, Arrieta JM, Herndl GJ (2006) Microbial diversity in the deep sea and the underexplored “rare biosphere”. *Proceedings of the National Academy of Sciences of the United States of America* **103**, 12115–12120.
- Stam MC, Mason PRD, Pallud C, Van Cappellen P (2010) Sulfate reducing activity and sulfur isotope fractionation by natural microbial communities in sediments of a hypersaline soda lake (Mono Lake, California). *Chemical Geology* **278**, 23–30.
- Stam MC, Mason PRD, Laverman AM, Pallud CL, Cappellen PV (2011) $^{34}\text{S}/^{32}\text{S}$ fractionation by sulfate-reducing microbial communities in estuarine sediments. *Geochimica et Cosmochimica Acta* **75**, 3903–3914.
- Starinsky A (1974) Relation between Ca-chloride brines and sedimentary rocks in Israel. Ph.D. thesis. The Hebrew University, Jerusalem (in Hebrew).
- Steinhorn I (1985) The disappearance of the long-term meromictic stratification of the Dead Sea. *Limnology and Oceanography* **30**, 451–462.
- Stokey LL (1970) Ferrozine- a new spectrophotometric reagent for iron. *Analytical Chemistry* **42**, 779–781.
- Thauer RK, Shima S (2008) Methane as fuel for anaerobic microorganisms. *Annals of the New York Academy of Sciences* **1125**, 158–170.
- Turchyn A, Sivan O, Schrag D (2006) Oxygen isotopic composition of sulfate in deep sea pore fluid: evidence for rapid sulfur cycling. *Geobiology* **4**, 191–201.
- Van der Wielen PWJJ, Heijs SK (2007) Sulfate reducing prokaryotic communities in two deep hypersaline anoxic basins in the Eastern Mediterranean deep sea. *Environmental Microbiology* **9**, 1335–1340.
- Westrich JT (1983) The consequences and controls of the bacterial sulfate reduction in marine sediments. Ph.D. dissertation, Yale University.
- Whitcar MJ, Faber E, Schoell M (1986) Biogenic methane formation in marine and freshwater environments: CO_2 reduction vs. acetate fermentation-isotope evidence. *Geochimica et Cosmochimica Acta* **50**, 693–709.
- Whitcar MJ (1999) Carbon and hydrogen isotope systematics of bacterial formation and oxidation of methane. *Chemical Geology* **161**, 291–314.
- Worden RH, Smalley PC, Fallick AE (1997) Sulfur cycle in buried evaporates. *Geology* **25**, 643–646.
- Wortmann UG, Bernasconi SM, Böttcher ME (2001) Hypersulfidic deep biosphere indicates extreme sulfur isotope fractionation during single-step microbial sulfate reduction. *Geology* **29**, 647.
- Wortmann UG, Chernyavsky B, Bernasconi SM, Brunner B, Böttcher ME, Swart PK (2007) Oxygen isotope biogeochemistry of pore water sulfate in the deep biosphere: dominance of isotope exchange reactions with ambient water during microbial sulfate reduction (ODP Site 1130). *Geochimica et Cosmochimica Acta* **71**, 4221–4232.
- Yecheili Y (2006) Response of groundwater system to change in the Dead Sea level. In: *New Frontiers in the Dead Sea Paleoenvironmental Research* (eds Enzel Y, Agnon A, Stein M). *Geological Society of America Special Papers* **401**, 113–126.
- Yecheili Y, Ronen D, Berkovitz B, Dershowitz W, Hadad A (1995) Aquifer characteristics derived from the interaction between water levels of a terminal lake (Dead Sea) and an adjacent aquifer. *Water Resources Research* **31**, 893–902.
- Yecheili Y, Shalev E, Wollman S, Kiro Y, Kafri U (2010) Response of the Mediterranean and Dead Sea coastal aquifers to sea level variations. *Water Resources Research* **46**, W12550.
- Zak I (1967) The geology of Mt. Sdom, Ph.D. thesis. The Hebrew University, Jerusalem (in Hebrew).